

1 **Community Workflows to Advance Reproducibility in**
2 **Hydrologic Modeling: Separating model-agnostic and**
3 **model-specific configuration steps in applications of**
4 **large-domain hydrologic models**

5 **W. J. M. Knoben¹, M. P. Clark^{1,2}, J. Bales³, A. Bennett⁴, S. Gharari⁵, C. B.**
6 **Marsh⁵, B. Nijssen⁶, A. Pietroniro⁷, R. J. Spiteri⁸, G. Tang¹, D. G.**
7 **Tarboton⁹, A. W. Wood¹⁰**

8 ¹Centre for Hydrology, University of Saskatchewan, Canmore, Alberta, Canada

9 ²Department of Geography and Planning, University of Saskatchewan, Saskatoon, Saskatchewan, Canada

10 ³Consortium of Universities for the Advancement of Hydrologic Science, Inc, Cambridge, Massachusetts,

11 USA

12 ⁴Hydrology & Atmospheric Sciences, University of Arizona, Tucson, Arizona, USA

13 ⁵Centre for Hydrology, University of Saskatchewan, Saskatoon, Saskatchewan, Canada

14 ⁶Civil and Environmental Engineering, University of Washington, Seattle, Washington, USA

15 ⁷Schulich School of Engineering, Department of Civil Engineering, University of Calgary, Calgary,

16 Alberta, Canada

17 ⁸Department of Computer Science, University of Saskatchewan, Saskatoon, Saskatchewan, Canada

18 ⁹Utah Water Research Laboratory, Utah State University, Logan, Utah, USA

19 ¹⁰National Center for Atmospheric Research, Boulder, Colorado, USA

20 **Key Points:**

- 21 • Reproducible, transparent modeling increases confidence in model simulations and
22 requires careful tracking of all model configuration steps
- 23 • We show an example of model configuration code applied globally that is traced
24 and shared through a version control system
- 25 • Standardizing file formats and sharing of code can increase efficiency and repro-
26 ducibility of modeling studies

Corresponding author: W. J. M. Knoben, wouter.knoben@usask.ca

Abstract

Despite the proliferation of computer-based research on hydrology and water resources, such research is typically poorly reproducible. Published studies have low reproducibility due to incomplete availability of data and computer code, and a lack of documentation of workflow processes. This leads to a lack of transparency and efficiency because existing code can neither be quality controlled nor re-used. Given the commonalities between existing process-based hydrological models in terms of their required input data and pre-processing steps, open sharing of code can lead to large efficiency gains for the modeling community. Here we present a model configuration workflow that provides full reproducibility of the resulting model instantiations in a way that separates the model-agnostic preprocessing of specific datasets from the model-specific requirements that models impose on their input files. We use this workflow to create large-domain (global, continental) and local configurations of the Structure for Unifying Multiple Modeling Alternatives (SUMMA) hydrologic model connected to the mizuRoute routing model. These examples show how a relatively complex model setup over a large domain can be organized in a reproducible and structured way that has the potential to accelerate advances in hydrologic modeling for the community as a whole. We provide a tentative blueprint of how community modeling initiatives can be built on top of workflows such as this. We term our workflow the “Community Workflows to Advance Reproducibility in Hydrologic Modeling” (CWARHM; pronounced “swarm”).

1 Introduction

Confidence in published findings depends on the reproducibility of the experiments and analyses that support these findings. In computational Earth System sciences research, reproducibility requires knowledge of the computer code and data that underpin a given manuscript. Such computer code can range from a few lines of code that are used to turn data into figures or compute certain statistical properties of the data, to modern process-based hydrologic models that can contain many thousands of lines of code. Despite encouraging progress in journal policies (Blöschl et al., 2014; Clark, Luce, et al., 2021), it is still difficult to reproduce published findings in the hydrologic sciences (Hutton et al., 2016; Stagge et al., 2019). Stagge et al. (2019) estimate that results may only be reproducible for between 0.6% to 6.8% of nearly 2000 peer-reviewed manuscripts published in six hydrology and water resources journals, due to a lack of sufficiently clearly described methods and a lack of the necessary input data or processing code.

In complex process-based hydrologic model applications, one additional barrier to reproducibility is the effort required to configure the model. It is not uncommon to hear claims that in such modeling studies 80% of overall effort is spent on configuring the model for a specific use case, and only 20% of overall effort is spent on using the model to answer research questions (e.g., Table 2.8 in Miles, 2014). Model configuration efforts are spent on assembling appropriate data sources for meteorological forcing data and geospatial parameter fields, wrangling these data into the specific format required by the model, defining appropriate model settings, and specifying the required computational infrastructure (e.g., finding the right collection of software libraries, installing or compiling the model, creating the required scripts to run the model). Additional time costs arise from dealing with the subjectivity in defining appropriate computational sub-domains (such as where to draw the boundaries for Hydrologic Response Units (Flügel, 1995)), interpreting soil and land cover maps, aggregating geospatial data into some form of representative value for a computational unit, and the associated iterative model configuration and testing steps. This model configuration process is typically poorly documented and extremely time-consuming. In short, the reproducibility problem for process-based hydrologic modeling occurs in part because of the lack of efficiency in model configuration tasks.

78 Reproducibility of computational science can be improved by following certain rec-
79 ommended best practices for open, accessible, and reproducible science (e.g., Gil et al.,
80 2016; Hutton et al., 2016; Sandve et al., 2013; Stodden & Miguez, 2013). Most focus is
81 currently on advancing the FAIR principles, which state that data, code, and methods
82 must be Findable, Accessible, Interoperable, and Reusable (Wilkinson et al., 2016). Re-
83 producibility requires FAIR data, but also includes sharing details about hardware, soft-
84 ware versions, and data versions (Añel, 2017; Bast, 2019; Hut et al., 2017; Sandve et al.,
85 2013). The environmental modeling community is interacting with these prescribed best
86 practices in multiple ways. Choi et al. (2021) identify three ongoing main thrusts aimed
87 at making computational environmental science more open, reusable, and reproducible.
88 First, data and models are increasingly openly available online through services as GitHub,
89 Hydroshare, and institutional repositories. Second, computational environments are in-
90 creasingly recorded and standardized through container applications (e.g., Docker, Sin-
91 gularity) or in self-documenting notebooks. Third, Application Programming Interfaces
92 (APIs) such as the pySUMMA API (Choi, 2020; Choi et al., 2021) make interacting with
93 complex models or data increasingly easier. In practice however, most progress in FAIR
94 science is arguably on Accessibility, whereas the other aspects of FAIR have received less
95 attention.

96 A key issue is that little attention is devoted to efficient reproducibility of the full
97 modeling workflow, which includes data acquisition, data preprocessing, model instal-
98 lation, model runs and post-processing of simulations. Efficiency is promoted in a gen-
99 eral sense through freely shared code and packages that perform specific tasks in the mod-
100 eling chain (for example, see Slater et al., 2019, for an overview of R packages that can
101 be used to populate a modeling workflow), and with model-specific tools such as VIC-
102 ASSIST (Wi et al., 2017). Dedicated efforts to ensure end-to-end reproducibility of mod-
103 eling studies are less common. Exceptions are Leonard and Duffy (2013, 2014, 2016), who
104 provide an in-depth description of a web-based interface for data preprocessing and vi-
105 sualization of simulations from the PIHM model, geographically constrained to the United
106 States; Havens et al. (2019, 2020), who provide an end-to-end workflow for setting up,
107 running, and analyzing a physics-based snow model; Vorobevskii et al. (2020); Vorobevskii
108 (2022), who develop an R package that sets up a simple hydrologic model anywhere on
109 the planet for a given domain discretization shapefile provided by the user; and Coon
110 and Shuai (2022), who provide a Python-based tool to configure watershed models across
111 the United States. Compared to sharing a model’s input and output data (which would
112 also enable a study to be reproduced), sharing complete workflows can be more efficient
113 in terms of required storage space. A workflow also provides a transparent record of all
114 modeling decisions and enables a more broadly defined form of reproducibility in which
115 a study can be repeated for a different region, a different data set, or a different version
116 of the same model to see if the original conclusions still hold.

117 The examples mentioned in the previous paragraph show that it is possible to doc-
118 ument workflows for a specific model (or, perhaps more accurately, for a specific version
119 of a model). A further challenge is in designing workflows in such a way that parts of
120 a workflow that configures Model A can be re-used in a workflow that configures Model
121 B. We refer to such a design as separating the model-agnostic and model-specific parts
122 of model configuration (see also Miles, 2014; Miles & Band, 2015, for an example of this
123 concept using EcoHydroLib for general data preprocessing and RHESysWorkflows for
124 creating model-specific input files applied to small watersheds across the CONUS and
125 Australia). In the case of process-based hydrologic modeling, models such as VIC (Hamman
126 et al., 2018; Liang et al., 1994), MESH (Pietroniro et al., 2007), SUMMA (Clark et al.,
127 2015a, 2015b; Clark, Zolfaghari, et al., 2021) and SVS (Husain et al., 2016) can be dif-
128 ferent in how they discretize the modeling domain, the physical processes they include,
129 and the equations used to describe a given process. However, at their core, these mod-
130 els are designed to solve the same general water and energy conservation equations (Clark,
131 Zolfaghari, et al., 2021).

132 Consequently, the data requirements for a myriad of extant hydrologic models will
133 vary in the specifics, but are similar in a general sense. In particular, process-based hy-
134 drologic models have similar needs for meteorological forcing data and geospatial param-
135 eter fields. Preprocessing of these similar data requirements does not need to rely on specifics
136 of the models themselves. For example, in the case of satellite-based MODIS land cover
137 data, model-agnostic steps are (1) downloading the source data, (2) stitching the source
138 data together into a coherent global map, (3) projecting this map into the Coordinate
139 Reference System of interest, (4) subsetting from the global data only the domain of in-
140 terest, and (5) mapping the resulting data in pixels onto model elements. Model-specific
141 steps would be to convert the resulting information (i.e., which pixels/land classes are
142 present per model element) to the specific format a model requires (e.g., storing the most
143 common land class per model element as a value in a netCDF file which the model reads
144 during initialization), and, if necessary, perform some form of data transformation to con-
145 nect land class data to model parameter values or settings (e.g., by defining a lookup ta-
146 ble that contains parameter values for each land cover type). Community-wide efficiency
147 gains are possible if workflows distinguish between model-agnostic and model-specific
148 steps and enable straightforward re-use of the workflow for model-agnostic steps (see also
149 Essawy et al., 2016; Gichamo et al., 2020, who make this argument in the context of web-
150 based model configuration tools).

151 The previous discussion leads us to conclude that the hydrologic modeling com-
152 munity can substantially improve how it shares model configuration code across mod-
153 eling groups. The key issue is that model physics code is increasingly distributed under
154 open-source licenses but the code that creates the necessary model inputs is typically
155 neither well-documented nor available without contacting the model developers. To move
156 towards a culture of community Earth System modeling, we define three distinct steps:

- 157 1. For a given model, model configuration code should be publicly available and di-
158 vided into model-agnostic and model-specific steps;
- 159 2. The configuration workflows of multiple different models, ideally using different
160 data sets, should be integrated into a proof-of-concept of a generalized model con-
161 figuration workflow;
- 162 3. A community-wide collaborative effort should refine the proof-of-concept into a
163 flexible model configuration framework.

164 The purpose of this paper is to introduce an open-source model configuration work-
165 flow that enables full reproducibility of a process-based hydrologic model setup for any
166 location on the planet, with the workflow code divided into model-agnostic and model-
167 specific parts. In other words, we perform the first of the three steps outlined above. This
168 advances our immediate goal of using this model configuration for a variety of projects
169 by reducing the time commitment needed to create model configurations for different do-
170 mains and by increasing confidence in the modeling outcomes due to increased transparency
171 and the possibility to reproduce results. Our broader goal is to foster a community mod-
172 eling culture within the Earth System sciences.

173 The workflow described in this manuscript contributes to this goal in two separate
174 ways. First, our code is openly accessible and therefore reusable by others who wish to
175 use all or part of it for their own experiments. Second, the documented lack of repro-
176 ducible hydrologic science (e.g., Stagge et al., 2019) suggests that there are barriers within
177 the hydrologic community to adopt more reproducible science. By providing a full ex-
178 ample of how a reproducible modeling study can be designed, we intend to lower at least
179 some of these barriers. A model-agnostic workflow approach, as proposed here, would
180 also conform directly to ISO 9001 requirements for quality assurance and quality con-
181 trol systems for software development, as the World Meteorological Organization (WMO)
182 describes in its guidance to WMO members on implementing a quality management sys-

183 tem for national meteorological and hydrological services (World Meteorological Organ-
184 ization, 2017).

185 The remainder of this paper is organized as follows. In Section 2, we outline sev-
186 eral high-level design considerations for reproducible modeling workflows and describe
187 how we implemented these principles in an example of such a workflow. The example
188 workflow uses open-source input data with global coverage, an open-source, spatially dis-
189 tributed, physics-based hydrologic modeling framework (SUMMA; Clark et al., 2015a,
190 2015b; Clark, Zolfaghari, et al., 2021), and an open-source network routing model (mizuRoute;
191 Mizukami et al., 2016, 2021) to generate hydrologic simulations across multiple spatial
192 scales. Technical details about the models and a step-by-step description of the work-
193 flow code are given in Appendix A. In Section 3, we present three test cases, covering
194 large-domain (global, continental) and local-scale model configurations to show that a
195 single workflow can be used to configure experiments that vary in terms of spatial and
196 temporal resolution and coverage. In Section 4, we reflect on the current state of repro-
197 ducibility in large-domain hydrologic modeling, with particular focus on why existing
198 efforts have seen only limited uptake and outline a path forward.

199 2 Increasing efficiency and reproducibility in Earth System modeling

200 2.1 Workflow design considerations

201 The reproducibility of modeling studies can be improved through openly published
202 workflows that track all decisions made during model configuration. We propose four gen-
203 eral guidelines for such model configuration workflows in the Earth System sciences. These
204 guidelines are informed by existing efforts to promote reproducibility and efficiency in
205 large-domain modeling efforts, and by our own experience with creating such large-domain
206 model configurations for process-based hydrologic models. We consider challenges for novice
207 and advanced modelers. Briefly, our recommendations are as follows:

- 208 1. **Separate model-agnostic and model-specific tasks.** The steps in the work-
209 flow must remain model-agnostic for as much of the workflow as possible and pro-
210 vide outputs in standardized, commonly used data formats. This increases the po-
211 tential utility of the code base for use in different projects and for users of differ-
212 ent models.
- 213 2. **Clarity for modelers.** The workflow must be easily accessible and usable in its
214 default form. A clear structure of the code accompanied by accurate documen-
215 tation and in-line comments increase the ease-of-use for novice and advanced mod-
216 elers alike.
- 217 3. **Modularity encourages use beyond the original application.** Customiza-
218 tion of the workflow must be possible and easy. This makes it possible to adapt,
219 improve, or change specific parts of the workflow to access new data sets, use new
220 processing algorithms, or target different models.
- 221 4. **Traceability is key.** Every outcome of each step in the workflow must be accom-
222 panied by metadata that describe the configuration code that generated the out-
223 come. This guarantees that, even if changes are made to the model configuration
224 code, any workflow outcome can still be traced back to its original settings.

225 In Section 2.2 we discuss an example of a model configuration workflow based on
226 these design considerations. In Section 2.3 we first provide a general description of model
227 configuration steps and then expand on each of the four points outlined above.

2.2 An example workflow for large-domain hydrologic modeling

2.2.1 Workflow description

Based on the design considerations listed in Section 2.1, we created a model configuration workflow for the Structure for Unifying Multiple Modeling Alternatives (SUMMA; Clark et al., 2015a, 2015b; Clark, Zolfaghari, et al., 2021) hydrologic model and the mizuRoute routing model (Mizukami et al., 2016, 2021). Briefly, SUMMA is a process-based, spatially-distributed hydrologic model that can be used to simulate the water and energy balance for given locations in space. mizuRoute is a vector-based routing model that can be used to route runoff from a hydrologic or land surface model through a river network. Detailed descriptions of both models can be found in Section A1. We selected both models for their flexible nature, computational capacity to model very large domains and availability of local expertise. Implementing configuration code for specific models (i.e., SUMMA and mizuRoute) in a generalized workflow, as we describe in this paper, is the first step on a possible path towards a community modeling culture that we outline in the Introduction.

Figure 1 provides a high level overview of our workflow in five key steps:

1. Workflow preparation, where workflow settings are defined and the necessary folder structures are generated;
2. Model-agnostic preprocessing, accomplishing data preparation steps that do not rely on any characteristics of the models being used. Data resulting from this step can thus be used for multiple different models;
3. Remapping of prepared data onto model elements. This step is listed as optional because not all models need this step;
4. Model-specific preprocessing to create model input files based on the prepared data sources, and generate model simulations;
5. Analysis and visualization to summarize model simulations into statistics and figures.

Progressively more detailed overviews of model-agnostic and model-specific tasks can be found in Appendix A2 and Figures A2, A3 and A4. Despite the seemingly large number of model-specific tasks in those figures, the time costs (in terms of code development) are larger for the model-agnostic tasks. The design considerations presented in this section and our implementation of them as described in Section 2.3 are comparable to existing efforts in the field of eco-hydrology involving the EcoHydroLib, RHESysWorkflows and HydroTerre tools (Miles, 2014; Miles & Band, 2015; Leonard et al., 2019; Choi, 2021), suggesting that this is a logical way to organize modeling workflows.

2.2.2 Workflow scope

The workflow scope deliberately excludes spatial discretization and parameter estimation (Figure 2). The scope of our workflow implementation assumes that the user has access to a basin discretization stored as an ESRI shapefile that defines the area of interest as discrete modeling elements (e.g., grid cells, sub-basins). Such a discretization may be derived from digital elevation models (see e.g. TauDEM or the geospatialtools code base, Sazib, 2016; Tesfa et al., 2011; Chaney & Fisher, 2021), or obtained from existing basin discretization products, such as HydroBASINS (Lehner & Grill, 2013) or the MERIT Hydro basin delineation (Lin et al., 2019). Moreover, the workflow does not currently include fine-tuning of model parameter values through calibration or estimation from auxiliary data sources. These calibration methods require selecting from a wide variety of calibration algorithms, each with their own strengths and weaknesses (e.g., Arsenault et al., 2014), and an even wider variety of objective functions that express the (mis)match between a model's simulations and observations of hydrologic states and fluxes

277 (e.g., Murphy, 1988; Clark, Vogel, et al., 2021; Gupta et al., 2008; McMillan, 2021; Mizukami
278 et al., 2019; Nash & Sutcliffe, 1970; Olden & Poff, 2003; Pushpalatha et al., 2012), re-
279 lying on a variety of further choices related to spatial scaling (e.g., Samaniego et al., 2010),
280 regionalization (e.g., Bock et al., 2015) and regularization of the calibration problem (e.g.,
281 Doherty & Skahill, 2006). These model calibration choices are not easily standardized
282 and require auxiliary data in the form of observations that are not readily available glob-
283 ally. The modular nature of our workflow implementation allows methods for basin dis-
284 cretization and parameter estimation to be integrated easily into our existing code base,
285 but doing so is planned for future work in an attempt to keep the scope of this first work-
286 flow example manageable.

287 **2.2.3 Workflow execution**

288 We present this workflow as a collection of Bash and Python scripts, stored inside
289 a folder structure that clearly indicates the appropriate order in which the scripts should
290 be executed (see Section 4.2.3 for a discussion of the choice to use scripts instead of other
291 options). The latest version of the workflow is available through GitHub: [https://github](https://github.com/CH-Earth/CWARHM)
292 [.com/CH-Earth/CWARHM](https://github.com/CH-Earth/CWARHM). The GitHub repository also contains further documentation
293 that helps a user set up the required computational environment and provides succinct
294 explanations of the purpose of various scripts, decisions and assumptions in cases where
295 such explanations are necessary. Lastly, the repository contains the basin discretization
296 used for our third test case that divides the upper part of the Bow River basin (Alberta,
297 Canada) into discrete modeling elements, so that users have immediate access to all the
298 materials needed to implement our workflow.

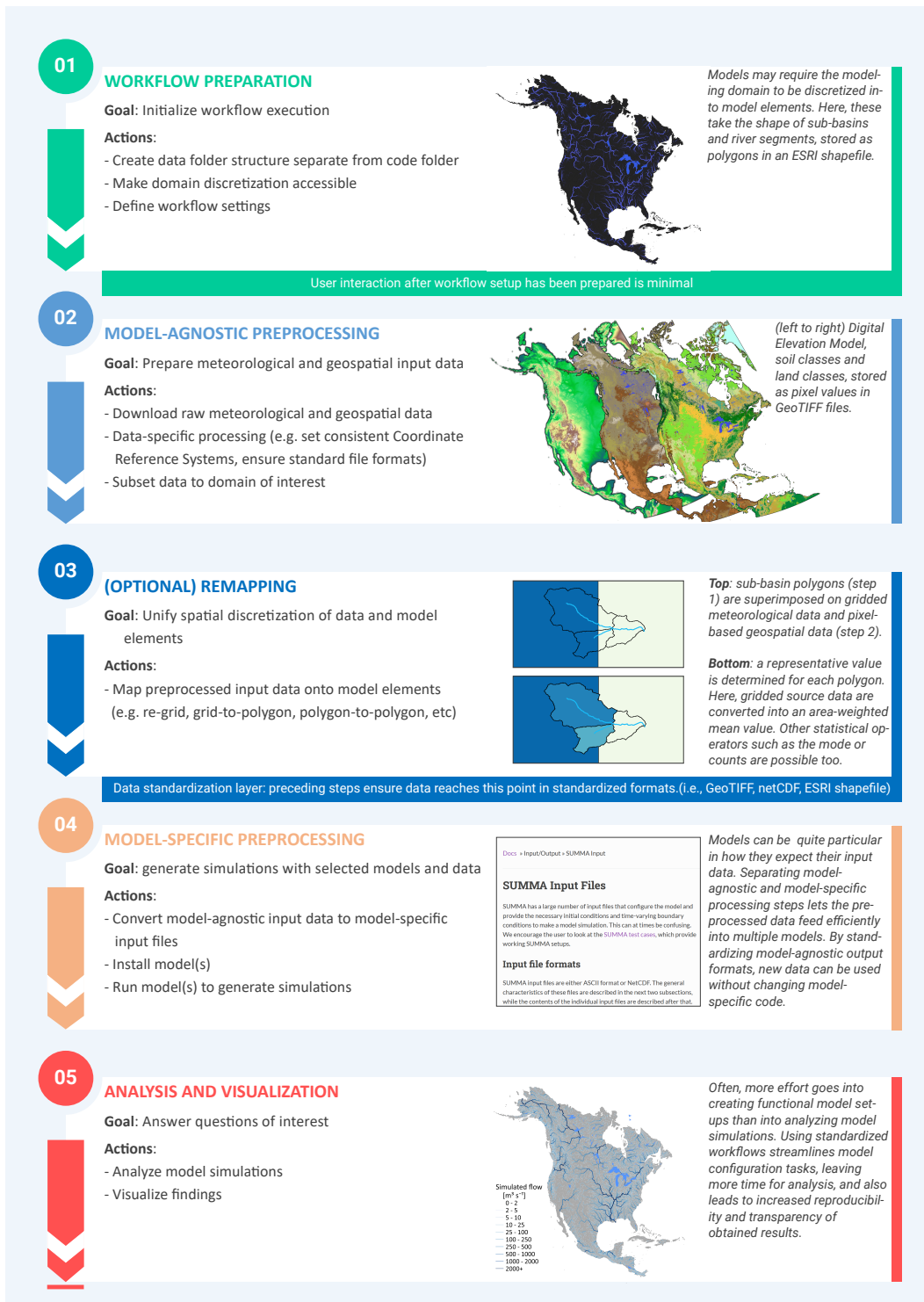


Figure 1. High-level overview of a workflow that separates model-agnostic and model-specific tasks. Model-agnostic tasks are shown in blue and model-specific tasks are shown in orange and red. A similarly high-level but more technical flowchart of such a workflow, using SUMMA (a process-based hydrologic model) and mizuRoute (a routing model) as example models, can be found in Figure A2. Technical details of our implementation of model-agnostic and model-specific processing steps can be found in Figures A3 and A4 respectively.

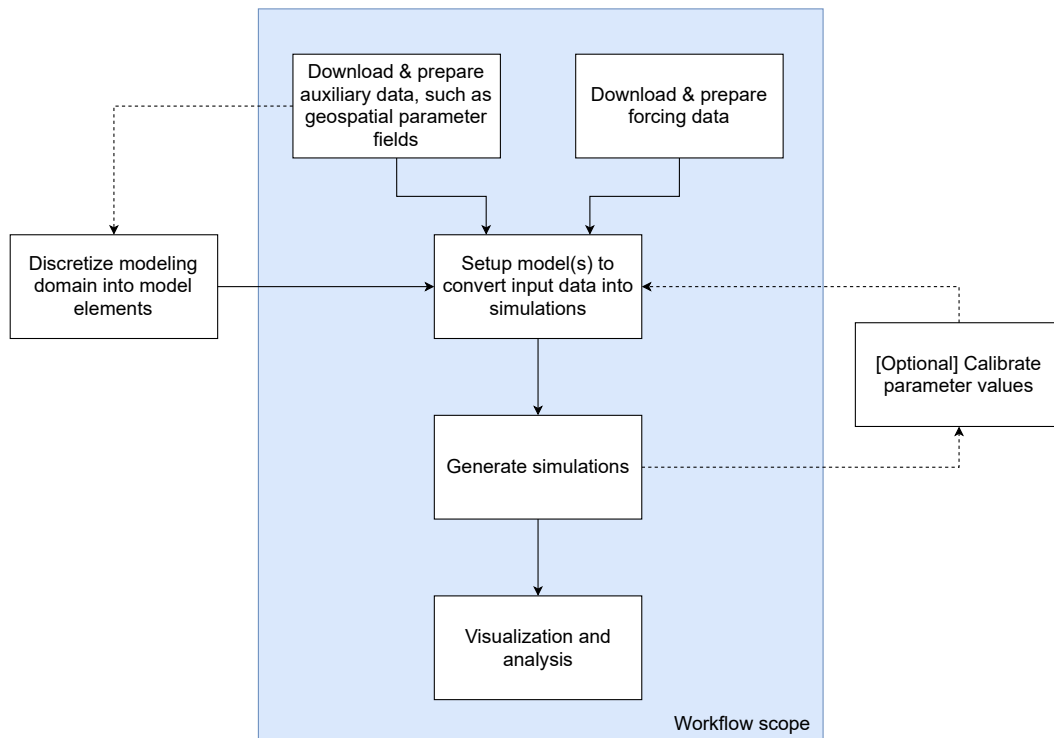


Figure 2. Schematic overview of a typical modeling workflow, with the scope of the example workflow described in this paper shown by the colored box. Dashed lines indicate potential connections between elements (such as geospatial parameter fields informing basin discretization, and parameter calibration feeding back into the model setup step where parameters for a new run are defined) that are not yet included as part of our workflow.

299 2.3 Implementation of workflow design recommendations

300 2.3.1 *Separate model-agnostic and model-specific tasks*

301 Our first design principle recommends separating model-agnostic and model-specific
 302 tasks. Model-agnostic tasks (shown in blue in Figure 1; light grey in Figure A2 and Fig-
 303 ure A3) are those tasks that are the same regardless of the model being used, under the
 304 assumption that the model requires a given data input at all. In our workflow implemen-
 305 tation these tasks include the downloading of meteorological forcing data and geospa-
 306 tial parameter fields (i.e., a digital elevation model (DEM), soil classes and vegetation
 307 classes), in some cases clipping raw datasets to the domain of interest and mapping of
 308 these data onto model elements such as grid cells or catchments. Fully model-agnostic
 309 outputs in this example are netCDF (.nc) files of meteorological forcing data (i.e., grid-
 310 ded hourly data at 0.25° latitude/longitude resolution) and GeoTIFF (.tif) files of var-
 311 ious geospatial parameter fields.

312 Model-specific tasks (shown in orange and red in Figure 1; dark grey in Figure A2
 313 and Figure A4) involve installing the chosen models, transforming the pre-processed data
 314 into the specific format the model requires, and running the models. In our workflow im-
 315 plementation this involves finding the mean elevation, mode land class and mode soil class
 316 per model element and exporting certain information about the modeling elements (area,
 317 latitude and longitude location, slope of the river network, etc.) into the netCDF files
 318 our models expect.

319 Due to the complex nature of existing models and their long histories of develop-
 320 ment, certain tasks cannot be cleanly separated into model-agnostic and model-specific
 321 tasks. The mapping of prepared forcing data and geospatial parameter fields onto model
 322 elements (shown in dark blue in Figure 1; intermediate grey shade in Figure A2 and Fig-
 323 ure A3) is an example of such a task. Certain models run on the same spatial resolution
 324 as the forcing and/or geospatial data grid, or are able to ingest gridded data in their na-
 325 tive alignment and internally map these onto the required model discretization. In our
 326 case, this remapping must be done outside the models. In the case of forcing data, the
 327 model-agnostic output of meteorological forcing files are mapped onto the model elements
 328 (catchments in this case), resulting in catchment-averaged model forcing. Temperature
 329 time series are further modified with catchment-specific lapse rates to account for ele-
 330 vation differences between the forcing grid and model elements. In the case of param-
 331 eter fields, intersections between the model-agnostic GeoTIFF files and the shapefile of
 332 the modeling domain are generated. These intersections show how often each elevation
 333 level, soil class, and land class occurs in each model element. These processes cannot be
 334 called truly model-agnostic because some models do not require them, but neither are
 335 they fully model-specific. To ensure maximum usability for different models, workflows
 336 must therefore be as modular as possible so that modelers can mix and match from avail-
 337 able code to suit the particularities of their chosen model (i.e., our third design princi-
 338 ple, described later).

339 *2.3.2 General layout and workflow control*

340 Our second design principle prescribes an intuitive interface for hydrologic mod-
 341 elers. We recognize two elements here: first, the code and data structure must be clear
 342 and easy to understand. Second, interacting with the workflow must be straightforward.
 343 Our example implementation strives to achieve both of these goals through a clean sep-
 344 aration of code and data and the use of a single configuration file (hereafter referred to
 345 as a “control file”) that outlines high-level workflow decisions such as file paths, spatial
 346 and temporal extent of the experiment, and details about the shapefiles that contain the
 347 domain discretization. Using configuration or control files is common practice in soft-
 348 ware design applications (see e.g. Sen Gupta et al., 2015) and avoids the need to intro-
 349 duce hardcoded elements such as file paths and variable values in the code itself.

350 In a typical application of our example workflow, the user first creates a local copy
 351 of the code provided on our GitHub repository. We refer to this local code as the “code
 352 directory”. The user would then specify a path in the control file that specifies where
 353 workflow data (such as forcing and parameter data downloads, model input files and model
 354 simulations) will be stored. The workflow is set up to read this path from the control
 355 file, create the specified folder structure and store all data for a given modeling domain
 356 in the user-specified data folder (referred to as the “data directory”). This allows a clean
 357 separation between the workflow code itself and the data downloaded and preprocessed
 358 by the workflow code (Figure 3). The workflow’s default settings ensure that the data
 359 directory is populated with folders and subfolders with descriptive names, making nav-
 360 igation of the generated data clear.

361 Table 1 contains a subset of the information that is stored in the control file that
 362 defines the workflow settings for a model configuration for the Bow River at Banff, Canada
 363 (see Section 3 for a description of this test case). The control file contains the high-level
 364 information needed by the workflow, such as the name of the user’s shapefiles, the names
 365 of required attributes in each shapefile, the spatial extent of the modeling domain, the
 366 years for which forcing data should be downloaded, and file paths and names for all re-
 367 quired data. The workflow scripts read information from the control file as needed. Keep-
 368 ing all information in one place enables a user to quickly generate model configurations
 369 for multiple domains, without needing to scour all individual scripts for hardcoded file
 370 paths, domain extents, etc. For example, changing the simulation period for a given do-

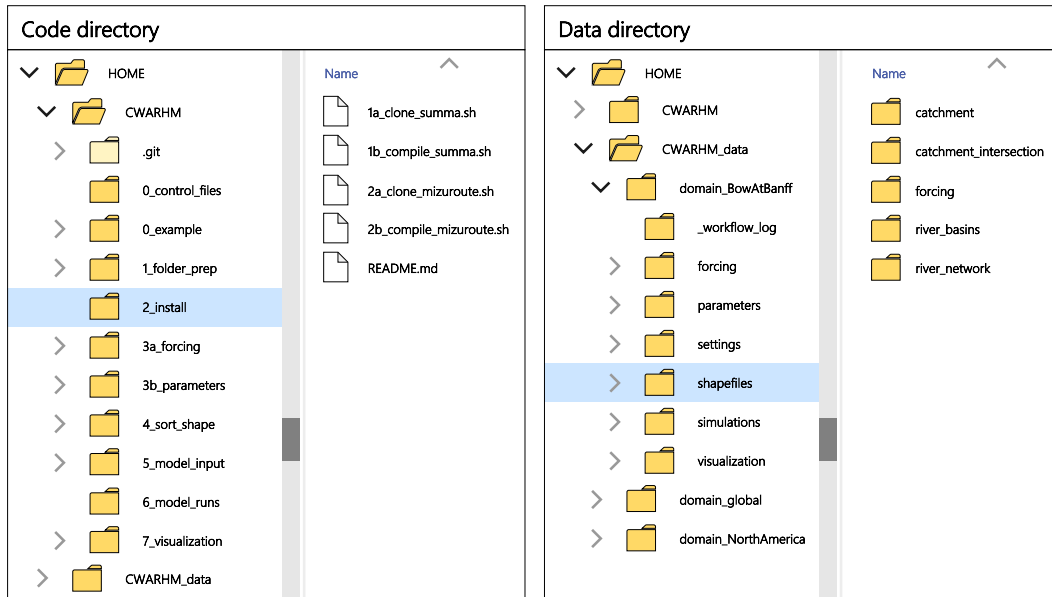


Figure 3. Example of separated code and data directories. The code directory (left) contains the scripts as available on the repository’s GitHub page. The data directory (right) contains the forcing data, parameter data, setting files, shapefiles and model simulations that are used and generated by the workflow code.

371 main requires changing two values in the control file, after which selected code can be
 372 re-run to download and preprocess the necessary forcing data and run new simulations.
 373 To configure our chosen models for a new domain (assuming that no changes to the model
 374 or desired data sets are introduced), a user only needs to provide a new domain discretiza-
 375 tion file and update in the control file the name of the domain (so that a new data folder
 376 can be generated), the names of the discretization files, and the bounding box of the new
 377 domain. The workflow can then be fully re-run to create a model configuration for the
 378 new domain, without any changes being made to the workflow scripts themselves.

379 *2.3.3 Flexibility at each step of model setup*

380 Our third design principle recognizes that process-based models are complex enti-
 381 tities and that the setup procedures for any given model are model- or even experiment-
 382 specific. Not all models will need to go through the same configuration steps, nor will
 383 every model experiment need the settings as defined in our example workflow. Our ex-
 384 ample workflow (Figure 1; details in Section A2) therefore aims to encourage adapta-
 385 tion beyond our original application through modularity and documentation.

386 First, we have chosen to present the workflow as a collection of scripts (i.e., the work-
 387 flow code is stored in simple text files that can be executed from the command line) rather
 388 than a Python package, R library, executable module or similar, so that the user has straight-
 389 forward access to the workflow code. This presentation simplifies adapting the code to
 390 different models or experiments by lowering the skill threshold needed to make adapta-
 391 tions to our code base, and is likely closer to the ways in which model configuration is
 392 currently often done. Second, the workflow separates model setup into numerous small
 393 tasks (see Figures A2 -A4) and saves all intermediate results to files. This modularity
 394 makes it straightforward to branch out from our chosen defaults at any given step in the
 395 modeling workflow. Third, for this iteration of our workflow, we have chosen to move

Table 1. Example of part of a workflow control file, showing settings for the Bow at Banff test case (see Section 3; actual control file available on the GitHub repository - see the Section “Open Research” at the end of this manuscript). These control files are simple text files containing three columns. The “Setting” column contains specific strings that each script in the repository looks for to identify which line in the control file contains the information the script needs. The “value” column contains the actual information, such as file paths, names of shapefiles and shapefile attributes, etc. Descriptions of each field are included for the user’s benefit but not used by the setup scripts. The benefit of collecting all information and settings in a single file is that it avoids hard-coding this information in the workflow itself, making it straightforward to apply the same workflow for a new experiment by simply updating the control file.

Setting	Value	Description
Modeling domain settings		
root_path	/user/CWARHM.data	Root folder where data will be stored.
domain_name	BowAtBanff	Used as part of the root folder name for the prepared data.
Settings of user-provided catchment shapefile		
catchment_shp_path	default	If 'default', uses 'root_path/domain_[name]/shapefiles/catchment'.
catchment_shp_name	bow_dist_elev_zone.shp	Name of the catchment shapefile. Requires extension '.shp'.
catchment_shp_gruid	GRU_ID	Name of the GRU ID column (can be any numeric value, HRU’s within a single GRU have the same GRU ID).
catchment_shp_hruid	HRU_ID	Name of the HRU ID column (consecutive from 1 to total number of HRUs, must be unique).
catchment_shp_area	HRU_area	Name of the catchment area column. Area must be in units [m^2].
catchment_shp_lat	center_lat	Name of the latitude column. Should be a value representative for the HRU.
catchment_shp_lon	center_lon	Name of the longitude column. Should be a value representative for the HRU.
Forcing settings		
forcing_raw_time	2008,2013	Years to download: Jan-[from],Dec-[to].
forcing_raw_space	51.7/-116.5/50.9/-115.5	Bounding box of the shapefile: lat_max/lon_min/lat_min/lon_max. Will be converted to ERA5 download coordinates in script. Order and use of '/' to separate values is mandatory.
forcing_time_step_size	3600	Size of the forcing time step in [s].

high-level decisions into the control file and leave various modeling decisions as assumptions in the workflow scripts. We have spent considerable effort on documenting any such assumptions (see Section A2) to let advanced users make targeted changes to the workflow code. Examples of these decisions include the number of soil layers used across the modeling domain, values for the initial model states, and default routing parameters. In future versions of our workflow, such decisions may be moved to a dedicated experiment-control file.

2.3.4 Code provenance

Our fourth design principle relates to traceability. The decision to separate code and data directories potentially introduces a disconnect between code and data, and situations may arise where it is no longer clear which version of a given piece of code generated a particular piece of data. This can happen in cases where the workflow code is updated after having already been used to create (part of) a model configuration. Although the changes to the workflow code can be tracked through version control systems such as Git, it is much more difficult to trace which version of the code generated the data. Every script in our example workflow therefore places both a log file and a copy of its code in the data sub-directory on which it operates. This ensures that, even if a user makes changes to the code directory, a record exists in the data directory of the specific code used to generate the files in that data directory. Copies of the model settings are stored in their simulation data directories by default so that simulation provenance can be traced as well.

3 Test cases

The test cases described in this section use the SUMMA and mizuRoute models. We refer the reader to Section A1 for details about both models and definitions of certain model-specific terms, such as Grouped Response Units (GRUs) and Hydrological Response Units (HRUs). For all test cases, meteorological input data are obtained from the ERA5 data set (Hersbach et al., 2020), elevation data are obtained from the MERIT Hydro data set (Yamazaki et al., 2019), land use data are obtained from the MODIS MCD12Q1 data set (Friedl & Sulla-Menashe, 2019), and soil data are obtained from the Soilgrids 250m data set (Hengl et al., 2017). Detailed descriptions of the input data can be found in Section A2.

3.1 Global model configuration

This first test case simulates hydrologic processes across planet Earth to illustrate the large-domain applicability of our approach. The global domain (excluding Greenland and Antarctica) is divided into 2,939,385 sub-basins or Grouped Response Units (GRUs; median GRU size is 36 km²; mean size is 45 km²) derived from the global MERIT basins data set (Lin et al., 2019). Simulations are run for a single month (1979-01-01 to 1979-01-31) at a 15-minute temporal resolution. Figure 4 shows summary statistics of several simulated variables. By design, we ran these simulations without a model spin-up period so that we might confirm our models function in regions where under typical conditions after model spin-up we would not expect to see much hydrologic activity (e.g., extremely water-limited regions). The value of this test case is to demonstrate that the workflow is applicable anywhere on the planet, and that the size of the model domain does not provide an insurmountable barrier to open and reproducible hydrologic modeling. The workflow documents every decision made during model configuration and enables repeatable simulations of this model domain with only a fraction of the original effort needed.

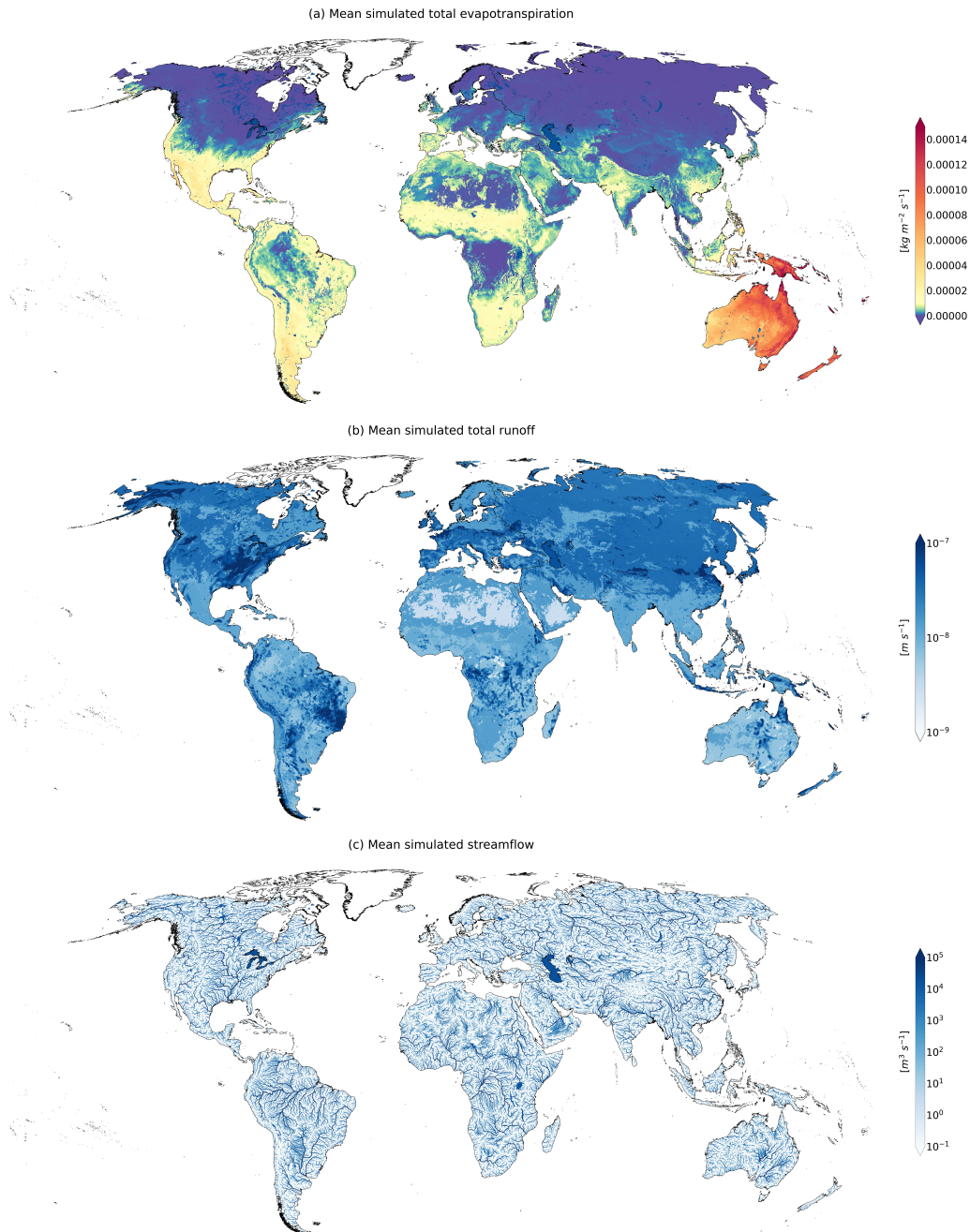


Figure 4. Overview of global simulations. SUMMA does not perform any computations for GRUs that are classified as being mostly open water, and mizuRoute was run without using its option to simulate routing through lakes and reservoirs. Lake delineations of lakes $> 100 \text{ km}^2$ are obtained from the HydroLAKES data set (Messenger et al., 2016) and used to mask open-water GRUs in this figure. Model setup uses default parameter values, and results are for illustrative purposes only. (a) Mean simulated total evapotranspiration, calculated as the sum of transpiration, canopy evaporation and soil evaporation. Note that the color scale has been designed to show global variability and local variability in Oceania simultaneously. (b) Mean runoff, calculated as the sum of surface runoff, downward drainage from the soil column, and lateral flow from the soil column. (c) Mean streamflow as determined by mizuRoute’s Impulse Routing Function approach.

443

3.2 Continental model configuration

444

445

446

447

448

449

450

451

452

453

454

455

456

457

458

459

460

461

This second test case uses 40 years of hourly forcing data to simulate hydrologic processes over the North American continent and illustrates the combined large-domain and multi-decadal applicability of our approach. The continental domain is divided into 517,315 sub-basins (median GRU size is 33 km²; mean size is 40 km²) derived from the global MERIT basins data set (Lin et al., 2019). Simulations are run from 1979-01-01 to 2019-12-31, again at a 15-minute temporal resolution. Figure 5 shows summary statistics of several simulated variables: as expected, snow accumulation tends to be higher in mountainous and higher-latitude locations; total soil water values are lower in the arid regions of the central and western US and Canada and northern Mexico; evapotranspiration rates fluctuate according to available energy (i.e., by latitude) and water; and large river networks are clearly visible as a result of accumulation of upstream river flow. These results are outputs from a model run with default process parametrizations and parameter values, and improvements to either or both will likely improve local model accuracy. However, the visible large-scale patterns appear hydrologically sensible and give us confidence that this initial model configuration is a solid basis for further model improvement and development. The modular nature of our workflow enables improvements to any single part of it without needing to change any other parts of the model configuration code, which contributes to increased efficiency in model improvement and use.

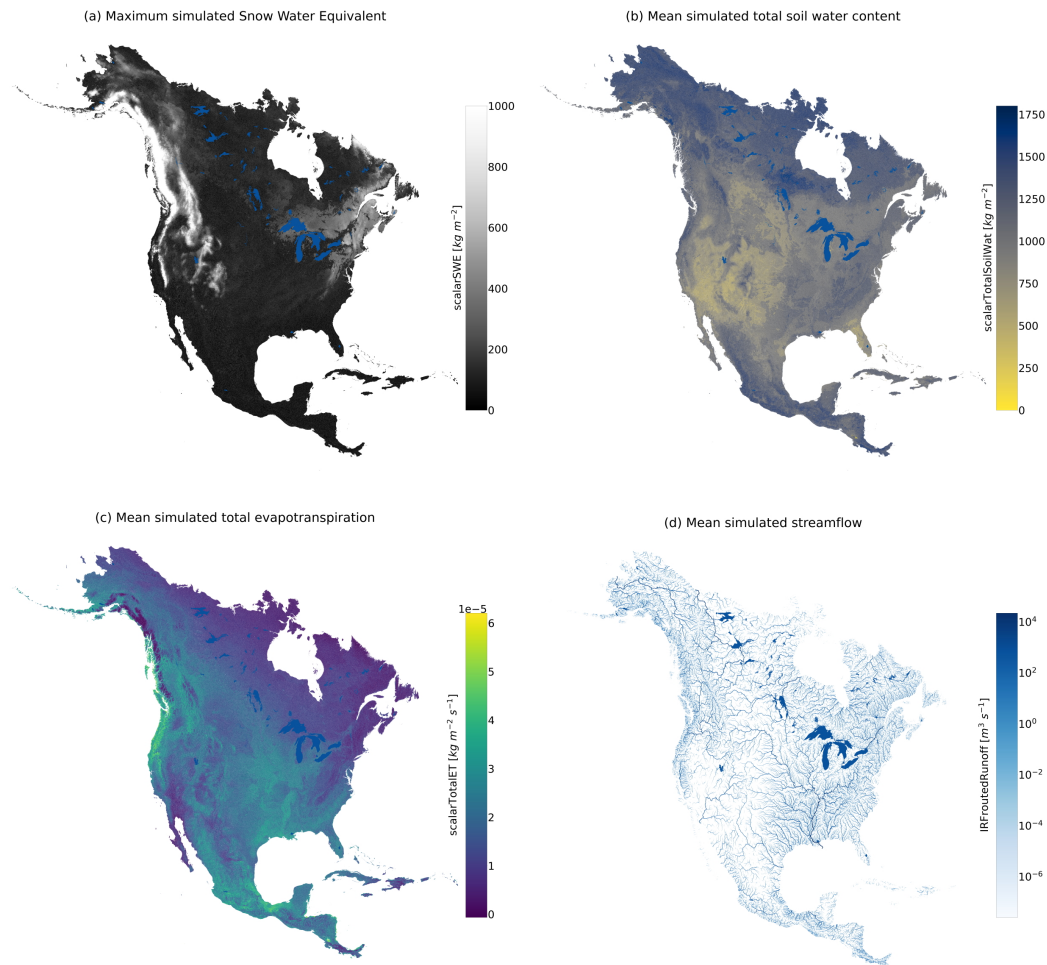


Figure 5. Overview of large-domain multi-decadal simulations. SUMMA does not perform any computations for GRUs that are classified as being mostly open water, and mizuRoute was run without using its option to simulate routing through lakes and reservoirs. Lake delineations of lakes $> 1,000 \text{ km}^2$ are obtained from the HydroLAKES data set (Messenger et al., 2016) and used to mask open-water GRUs in this figure. Model setup uses default parameter values, and results are for illustrative purposes only. (a) Maximum simulated Snow Water Equivalent per GRU is capped at $1,000 \text{ [kg m}^{-2}\text{]}$ for visualization purposes. (b) Mean simulated total soil water content, which includes both liquid and solid water in the soil profile. (c) Mean simulated evapotranspiration, defined as the sum of evaporation from the soil profile and the canopy, and transpiration by vegetation. (d) Mean streamflow as determined by mizuRoute's Impulse Routing Function approach.

462

3.3 Local model configuration

463

464

465

466

467

468

469

470

471

472

473

474

475

476

477

478

The modeling domain in the global and continental test cases is discretized into sub-basins (Grouped Response Units, GRUs, in SUMMA terminology) of roughly equal area. SUMMA uses a flexible spatial discretization approach that allows GRUs to be sub-divided in as many Hydrologic Response Units (HRUs) as the modeler thinks practical and relevant. These HRUs can be used, for example, to represent different elevation zones, differences in soil or land use, differences in topography, or a combination of several of these elements (see Section A1 for a more detailed explanation). As a more localized test case, we created a subset of the MERIT basins data set (Lin et al., 2019) that covers the Bow River from the Continental Divide to the town of Banff, Alberta, Canada. We then sub-divided each MERIT sub-basin (i.e. each GRU) into multiple HRUs based on 500m elevation increments (Figure 6a), created a new control file for this new domain, and reran the workflow code. No changes were necessary to any of the workflow scripts because the scripts obtain all the required information from the updated control file and the code is generalized to handle both the large-domain case, where GRUs are not sub-divided into HRUs, and this local case, where HRUs are used. Note that this local test case could be for any basin on the planet.

479

480

481

482

483

484

485

486

487

488

489

490

491

492

493

494

This third test case uses hourly forcing data from 2008-01-01 to 2013-12-31 (again run at a 15-minute sub-step resolution). Temperature lapse rates are applied to the forcing data for each individual HRU, meaning that the hydrometeorological conditions are somewhat different in each HRU despite the forcing grid cells being relatively large compared to the delineated catchments (see Figure A7). Figure 6b shows that simulated Snow Water Equivalent (SWE) varies per HRU and accumulated streamflow varies per stream segment. These figures provide a rudimentary test of the generated model setup for a location for which we have clear expectations about how the simulations should look (see also a cautionary note on the use of global data products in Appendix B). As may be expected, more snow accumulates at higher elevations, whereas the valley bottoms have a lower snowpack due to warmer air temperatures but larger flows due to their larger accumulated upstream area. As with the global and continental simulations, this local test case is fully reproducible and all model configuration decisions are stored as part of the workflow. This local test case also shows that different model configurations (in terms of spatial discretization in GRUs and HRUs) can be generated by the same model-specific workflow code.

495

4 Discussion

496

4.1 To what extent does our workflow fulfill reproducibility requirements?

497

498

499

500

501

502

503

504

505

506

507

508

509

Best practices for open and reusable computational science can be briefly summarized as follows (e.g., Gil et al., 2016; Hutton et al., 2016; Stodden & Miguez, 2013): data must be available and accessible, code and methods must be available and accessible, active development on issues with data, code, and methods must be possible, and licensing of data and code should be as permissive as possible. These requirements are formalized in the FAIR principles (Findable, Accessible, Interoperable, Reusable; Wilkinson et al., 2016) but by themselves are not enough to guarantee reproducibility of computational science (e.g., Añel, 2017; Bast, 2019; Hut et al., 2017). To be fully reproducible, details about hardware, software versions, and data versions also need to be recorded and shared (e.g., Choi et al., 2021; Chuah et al., 2020; Essawy et al., 2020). Such practices require a certain time investments but the benefits are clear: the resulting science is more transparent, can be more easily reproduced, and follow-up work will be more efficient because less time is spent on mundane tasks such as data preparation.

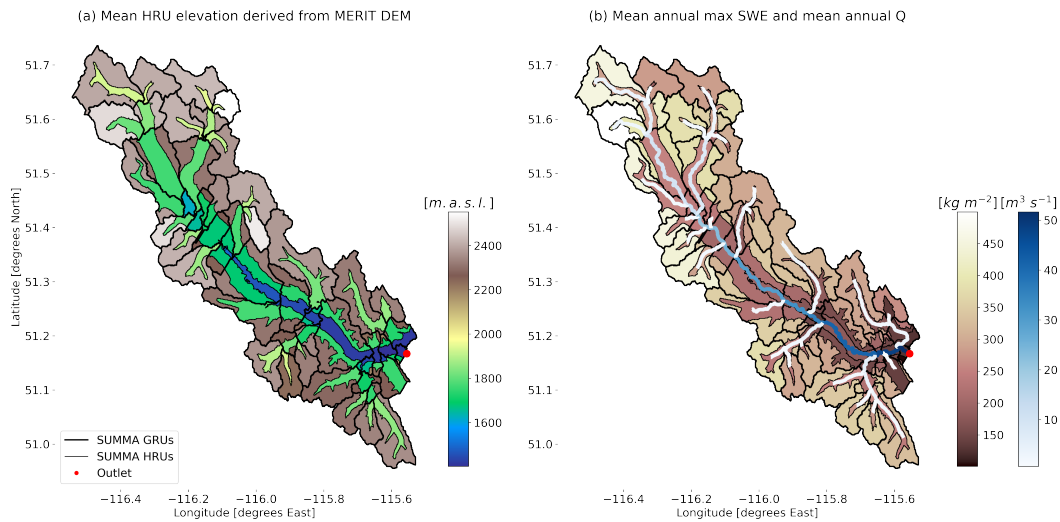


Figure 6. Overview of local simulations. Model setup uses default parameter values, and results are for illustrative purposes only. (a) Mean HRU elevation as derived from MERIT Hydro DEM. (b) Mean of maximum SWE per water year shown for each HRU, and mean annual streamflow shown for each river segment. Only data from complete water years is included.

510 Sandve et al. (2013) outline ten rules for reproducible computational science in the
 511 field of Computational Biology, and these are also applicable to Earth System model-
 512 ing. Our workflow follows nine of these guiding principles:

- 513 (1) Our workflow stores copies of the scripts that generate data together with the data
 514 itself, which allows a researcher to track how a given result was produced;
- 515 (2) Our workflow contains no manual data manipulation: all changes to the data are
 516 done in scripts and can be traced;
- 517 (3) An exact version of all software used is tracked, partly as installable Python en-
 518 vironments and partly on the workflow repository for command line utilities;
- 519 (4) All scripts are version controlled through Git;
- 520 (5) Our workflow is modular and stores intermediate results in individual folders to
 521 aid in debugging of setups and to allow easy diversion from our workflow;
- 522 (6) All data that may support analysis and figures are systematically stored in a log-
 523 ical folder structure;
- 524 (7) Our chosen model structure is flexible in prescribing outputs, removing a need to
 525 modify the model source code to display specific results;
- 526 (8) Our visualization code keeps a precise record of which results file contains the data
 527 that underpin a given figure and thus a record exists of which data support a given
 528 textual statement about the analysis;
- 529 (9) The workflow code is publicly accessible.

530 Their tenth principle, keeping accurate note of the seeds that underpin any element
 531 of randomness in the analysis, does not apply here. Sandve et al. (2013) also recommend
 532 sharing access to simulation results. This can be done through repositories such as Hy-
 533 droShare or Pangaea but may be infeasible in the case of large-domain Earth System mod-
 534 eling. For example, storing all input and output data of our continental test case takes
 535 approximately 13 TB.

Internal tests on different hardware and by different researchers indicate that our workflow effectively implemented these principles for open and reproducible science in practice: the workflow can be used to generate identical model inputs and outputs by specifying exact library, package, and model versions. Some caveats apply, however. Although it is possible to trace model source code versions through Git commit IDs, such IDs can obviously not account for local code modifications that are not tracked through Git. Good “computational lab hygiene” is needed to ensure consistency between what is reported to have been done and what has in fact been done. Further, not all data sets that underlie our model setups have Digital Object Identifiers assigned to specific versions of the dataset. Given the size of the data sets involved, sharing the data itself is infeasible, and some care must be taken to precisely track when data were downloaded as a means of making the use of data without DOIs traceable. Last, reproducibility is ensured through specifying exact versions of packages and libraries but many of these packages and libraries are undergoing rapid development and new versions are released frequently. There is a potential issue for reproducibility if older software versions for one reason or another are no longer available (though for fully open-source software this should theoretically not happen). New versions of specific software may however become incorporated into a new version of a workflow if they provide some needed functionality. To ensure backward compatibility, such new workflow versions must therefore also be assigned a new DOI so that any specific workflow version can be tracked and re-used when needed.

4.2 Towards community modeling

4.2.1 *Short-term benefits of using workflows*

This paper introduces a modular model configuration workflow that separates model-agnostic and model-specific configuration steps. The two main benefits of approaching environmental modeling from this angle are clear: configuring multiple modeling experiments becomes much more efficient, and results are reproducible, because all model configuration decisions can be traced. These benefits address two problems that currently affect Earth System modeling. First, creating a typical model configuration is both difficult and time consuming, and it is possible that model configuration tasks do not receive the attention they deserve. Code may not be checked as thoroughly as may be necessary because bugs may not be readily apparent, and any time spent on model configuration is consequently not spent on writing journal articles or meeting report deadlines. Configuring models can be more efficient if model configuration code is freely and openly shared. This enables time that is currently spent on creating model configurations to instead be spent on in-depth analysis, improving the model representation of real-world processes, and fixing any bugs that may be found in the configuration code or the model source code. If bugs are found, tracing the experiments that are affected by these bugs is possible, and it will be clear which studies need to be corrected. Openly shared model configuration code therefore has the potential to increase the robustness of model simulations and accelerate advances in modeling capabilities. Second, by publishing workflow code alongside a manuscript, the provenance of scientific results remains traceable (see e.g. Hutton et al., 2016; Melsen et al., 2017). This can increase confidence in model results. It also enables more effective follow-up studies because all decisions that underpin the original study can be found in the public domain.

4.2.2 *Long-term vision for community workflows*

We see workflows such as the one presented in this paper as the first step towards a community-wide modeling framework. Figure 7 illustrates an example of such a framework using the workflow code presented in this paper as examples of each framework layer (see also Miles, 2014). In addition to a division between model-specific and model-agnostic tasks, we envision a framework that distinguishes between data-specific and data-agnostic

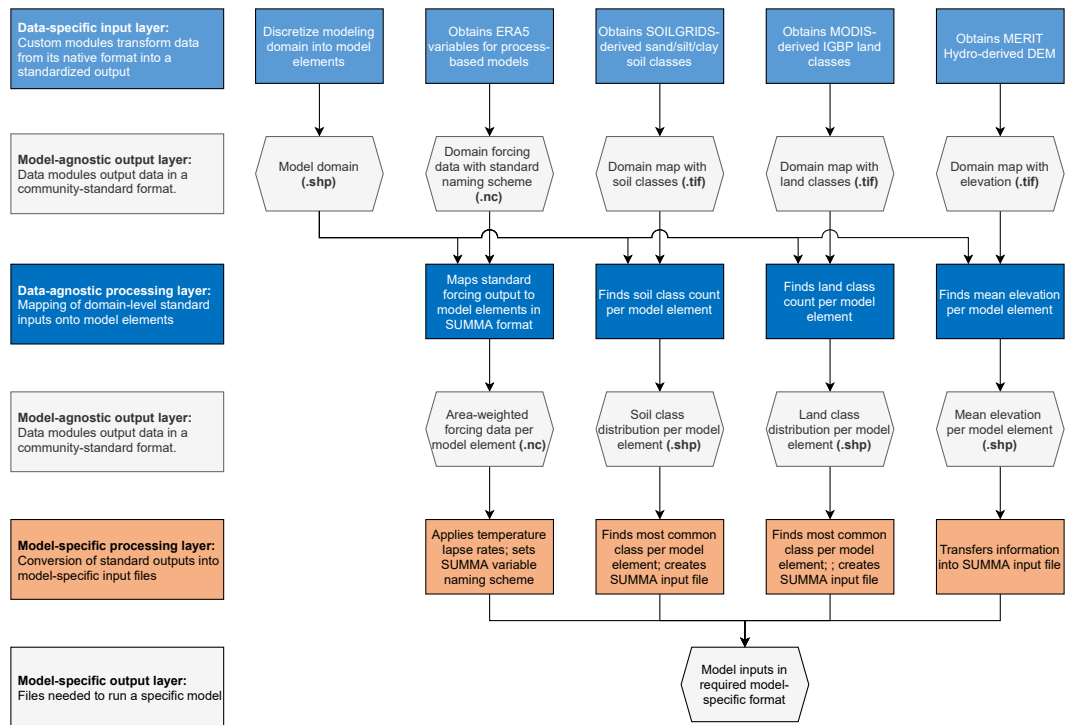


Figure 7. Schematic overview of a generalized community modeling framework, populated with examples from our SUMMA setup configuration workflow. Key to this modular approach is community-wide agreement on the formats used in each model-agnostic standardization layer. Such standards enable a modular approach to model-configuration, where existing modules can be seamlessly replaced, as long as they are designed to read and output data in the agreed-upon formats.

587 preprocessing steps. Processing layers would be separated by standardization layers that
 588 prescribe the output format for the preceding processing layer and consequently the input
 589 format for the following processing layer (see also Miles, 2014, where the use of common
 590 file types is discussed as a recommended approach between the model-agnostic and
 591 model-specific parts of workflows). Community-wide agreement on the formats used in
 592 standardization layers will promote efficient interoperability of different data-specific pro-
 593 cessing modules, possibly as part of broader work on international hydrologic standards
 594 (e.g., HY_Features, Blodgett & Dornblut, 2018). Using our workflow as an example, we
 595 have created data-specific processing modules for ERA5 meteorological data, SOILGRIDS-
 596 derived soil classes, MODIS-derived land classes, and a MERIT Hydro-derived DEM.
 597 These modules generate data in standardized formats (in this case, netCDF4 forcing data
 598 and GeoTIFF spatial maps) that in turn feed into the data-agnostic remapping layer.
 599 This layer generates further model-agnostic data in netCDF4 and Shapefile formats that
 600 are then transformed into SUMMA’s inputs through a model-specific processing layer.

601 Our currently defined model-agnostic tasks are of course still implicitly SUMMA-
 602 centric (i.e., we have completed those tasks because they generate the data that SUMMA
 603 requires), though in principle the outputs can immediately be used by other models. The
 604 modular nature of our workflow makes adding new datasets and processing steps as straight-
 605 forward as writing new data-specific and data-agnostic routines and inserting them in
 606 a further unchanged workflow. Changing to a different model requires writing a new model-
 607 specific interface layer, but existing data processing scripts can remain untouched (again,

608 assuming that the new model has data needs that can be met by already existing data
 609 processing scripts). This means that the workflow can be tailored to a specific model or
 610 experiment in a fraction of the time needed to create the model configuration from scratch.
 611 The modified workflow can then be published alongside the new modeling results to keep
 612 those results traceable.

613 It is of course possible that our attempt to separate model tasks into model-agnostic
 614 and model-specific parts is not equally applicable to different models that are currently
 615 in use. In such cases, we hope that providing a tangible example of how model config-
 616 uration code can be organized and shared in a structured way will nevertheless inspire
 617 others to create their own workflows. Modifying our workflow or adapting it for differ-
 618 ent purposes in such ways is the second step we anticipate as needed to move towards
 619 a community modeling paradigm. By creating new or modifying existing workflows for
 620 new experiments and models, the required structure of a generalized model setup work-
 621 flow may become apparent. As a third and final step, this generalized workflow can be
 622 formalized into a community-driven modeling framework that enhances efficiency and
 623 transparency in Earth System modeling.

624 To initiate the process of creating a community-driven modeling framework, our
 625 workflow is available as open-source code: <https://github.com/CH-Earth/CWARHM> (last
 626 access: 2022-07-27). We have chosen a permissive license (GNU GPLv3) that allows oth-
 627 ers to freely use and modify our code under the conditions that the modified code base
 628 is published under the same license, with attribution of its source and a list of changes.
 629 We envision a gradual process in which our repository is modified by others (either piece-
 630 meal or by incorporating our entire code base in a new repository as, for example, a Git
 631 submodule), increasingly more data-specific and models-specific processing capabilities
 632 are made public, and appropriate formats for standard file formats become apparent. De-
 633 ciding if and how to integrate these different elements into a single modeling framework
 634 is a decision the community will need to make in due course.

635 ***4.2.3 Where do workflows stand in the existing reproducibility landscape*** 636 ***in hydrologic modeling?***

637 We approach the workflow problem from a catchment modeling perspective within
 638 the wider Earth System modeling community (see the definitions of different commu-
 639 nities in Archfield et al., 2015). Calls for more efficient, transparent, and shareable model
 640 configuration approaches are not new in the catchment modeling community (see e.g.
 641 Blair et al., 2019; Famiglietti et al., 2011; Hutton et al., 2016; Tarboton et al., 2009; Weiler
 642 & Beven, 2015) and considerable progress along these lines has been made. For exam-
 643 ple, Sen Gupta et al. (2015) standardize model inputs and outputs to efficiently couple
 644 a snow accumulation and melt routine with an existing open source modeling framework;
 645 Ecohydrolib (Miles & Band, 2015; Miles, 2014; Miles et al., 2022) is a Python API that
 646 automatically preprocesses ecohydrologic parameter fields and forms the basis of a model
 647 configuration workflow for the RHESSys model; Bandaragoda et al. (2019) develop a gen-
 648 eral interface for building and coupling multiple models, using the Landlab toolkit (Hobley
 649 et al., 2017; Barnhart et al., 2020); Gan et al. (2020) integrate a web-based hydrologic
 650 model service with a data sharing system to promote reproducible workflows; HydroDS
 651 (Gichamo et al., 2020; Dash & Tarboton, 2022) is a web-based service that can be used
 652 to prepare input data for modeling; Bennett et al. (2018, 2020) create a tool to estimate
 653 hourly forcing input for physics-based models from commonly available daily data; Bavay
 654 et al. (2022) describe a tool that can be used to effectively create a Graphical User In-
 655 terface for a given model; Essawy et al. (2016) provide an example of how containeriza-
 656 tion (storing a full computational environment into a software container) enhances re-
 657 producibility; and Kurtzer et al. (2017, 2021) develop a means of saving and transfer-
 658 ring software and computing environments on and between High Performance Comput-
 659 ing clusters. Put together, most if not all elements for fully reproducible, easy-to-use,

660 computational hydrology already exist. So far, however, uptake of these tools is regret-
661 tably not widespread.

662 We speculate that uptake of existing tools is somewhat low for multiple reasons.
663 First, these tools are typically provided as self-contained packages where some form of
664 interface exists between the user and the source code. Such packages tend to be easy to
665 use for their intended purpose but take time to understand and do not necessarily pro-
666 vide much flexibility to deviate from their intended purpose. Layering additional func-
667 tions on top of an existing package or modifying a package's source code is certainly pos-
668 sible, but can be outside the comfort zone of many users. Second, several model-configuration
669 tools are provided as web-based services. This can be appealing because, for example,
670 data can be pre-downloaded to speed up model configuration and model simulations can
671 be easily shared. The advantage of such approaches is that they can be combined with
672 some form of server-side data transformations (e.g., subsetting or averaging), which min-
673 imizes data transfers. Storing the inputs for and outputs of large-domain simulations can,
674 however, be cumbersome, and keeping pre-downloaded data up-to-date and sufficient for
675 all user needs takes sustained, long-term effort. A further complication is that it is re-
676 grettably common that such web-based services require some form of manual interac-
677 tion with the webpage, limiting opportunities to automate data acquisition tasks. Third,
678 the lack of community agreement on standard data formats means that developers of new
679 tools typically decide to have their tool output data in a format relevant to their own
680 application, which may not be a format that is widely used by others. It is cumbersome
681 for developers to have their tools ingest multiple different data formats and such func-
682 tionality is therefore somewhat rare. Community-wide agreement on a set of standard
683 data formats, such as proposed in Figure 7, will make it easier for developers to know
684 which data formats their tools must be able to ingest and produce to guarantee seam-
685 less interaction with other existing tools.

686 In short, some of the existing tools may be overdesigned or unsuitable for where
687 the majority of the community currently stands. Such tools are typically designed by
688 a small group of people, using a proof of concept or test case that is directly applicable
689 to the developers' own work. Developers can make educated guesses about how their tool
690 can be made more general beyond their proof of concept, as we had to do here. Actu-
691 ally extending these proof of concepts typically relies on the original developers having
692 both the motivation and opportunity to implement functionality for others (e.g., incor-
693 porating new data sets or including model-specific layers for other models) or on new
694 developers being willing to first understand the existing package or web-service and then
695 modifying it.

696 Our approach to provide a tangible example of how to structure model configura-
697 tion tasks is different. First, our use of scripts that allow a user to immediately access
698 the workflow code is likely much more similar to how many models are currently con-
699 figured than if we had wrapped our workflow code in some form of user interface (such
700 as a Python package, R library, or web interface). This lowers the barrier to trying our
701 approach. Second, our use of standardization layers that require intermediate files to be
702 in commonly used data formats (GeoTIFF, netCDF, ESRI shapefiles) makes it easy to
703 adapt small parts of our workflow without needing to change any upstream or downstream
704 configuration tasks. Third, there are clear and immediate benefits of adopting a work-
705 flow approach of the type proposed in this paper that are unrelated to how widely (or
706 not) this approach is adopted: creating new configurations for the models used in such
707 workflows will be more efficient and the resulting science will stand on a firmer founda-
708 tion than closed-source results. Should our approach become more widely adopted, then
709 the path to a community modeling framework builds itself: as more examples of model
710 configuration workflows become available, our preliminary sketch of a community mod-
711 eling framework in Figure 7 can be refined or redrawn. The best approach to design, build,
712 and maintain such a community framework can be decided in due course, and appropri-

713 ate funding may be sought when needed. Advancing the paradigm of community mod-
 714 eling requires active participation of the community. By providing an example of a com-
 715 munity modeling workflow, we hope to encourage uptake, modification and adaptation
 716 of such community approaches.

717 4.3 Future work

718 We outlined three steps to move toward a culture of community modeling in the
 719 Earth sciences in Section 1:

- 720 1. For a given model, model configuration code should be publicly available and di-
 721 vided into model-agnostic and model-specific steps;
- 722 2. The configuration workflows of multiple different models, ideally using different
 723 data sets, should be integrated into a proof-of-concept of a generalized model con-
 724 figuration workflow;
- 725 3. A community-wide collaborative effort should refine the proof-of-concept into a
 726 flexible model configuration framework.

727 This manuscript provides an example of the first step in this list, by showing how
 728 configuration code for a single model can be implemented in a more general framework.
 729 Ongoing work focuses on the second step, by integrating multiple different models such
 730 as MESH (Pietroniro et al., 2007) and HYPE (Lindström et al., 2010; Arheimer et al.,
 731 2020) into our workflow by adding the necessary processing code for these models. This
 732 work is nearing completion, and both models have successfully been able to re-use the
 733 model-agnostic part of the code base described in this paper, suggesting that a ‘bottom-
 734 up’ kind of approach to community modeling is feasible.

735 New processing code naturally involves writing new model-specific routines that
 736 convert existing pre-processed data into the specific formats each new model needs. In-
 737 clusion of additional models also necessitates certain new model-agnostic processing rou-
 738 tines. For example, whereas SUMMA works on the assumption that a single computa-
 739 tional element has a single (possibly dominant) land cover type (but allows spatially flex-
 740 ible configurations so that each different land cover type can be assigned its own com-
 741 putational element), MESH lets the user specify a histogram of land cover types within
 742 each grid cell. Our current implementation of model-agnostic land cover remapping there-
 743 fore still follows the implicit assumption that the required processing output is a single
 744 land cover class per model element. A new routine is needed that returns the histogram
 745 of land classes per model element that MESH requires. Examples such as these show that
 746 a modular approach to a generalized community modeling framework as described in Sec-
 747 tion 4.2.2 and Figure 7, where new processing modules can be inserted without requir-
 748 ing changes to existing upstream and downstream routines, is a likely path forward on
 749 the road to community modeling.

750 5 Conclusions

751 This paper describes a code base that provides a general and extensible solution
 752 to configure hydrologic models. Specifically, the paper provides a tool that can be used
 753 to create reproducible configurations of the Structure for Unifying Multiple Modeling
 754 Alternatives (SUMMA, a process-based hydrologic model) and mizuRoute (a vector-based
 755 routing model). We consider this the implementation of a single model in a general frame-
 756 work that separates model-agnostic and model-specific configuration tasks. Such a sep-
 757 aration of tasks makes inclusion of new models in this framework relatively straightfor-
 758 ward because most of the data pre-processing code can remain unchanged and only model-
 759 specific code for the new model needs to be added.

760 The critical component of this framework are standardization layers, which pre-
 761 scribe the details of the file formats that must come out of the preceding processing layer
 762 and form the input of the following processing layer. By standardizing inputs and out-
 763 puts, the code that forms the processing layers only needs to concern itself with these
 764 prescribed formats. Changing specific processing modules to, for example, pre-process
 765 a different data set, perform a different way of mapping data onto model elements, or
 766 prepare input files for a different model, can therefore happen in isolation from the re-
 767 mainder of the workflow as long as the new processing code accepts and returns data in
 768 the prescribed formats. We show examples of this approach with global and multi-decadal
 769 continental SUMMA and mizuRoute simulations, and with a local SUMMA configura-
 770 tion that uses a more complex spatial discretization than the global and continental sim-
 771 ulations use.

772 Future work will involve adding model-specific code for multiple additional mod-
 773 els and any needed data-specific preprocessing modules. We have termed this initiative
 774 “Community Workflows to Advance Reproducibility in Hydrologic Modeling” (CWARHM;
 775 “swarm”) and we encourage others to be part of this model-agnostic workflow initiative.
 776 The configuration code for the SUMMA and mizuRoute setup shown in this manuscript
 777 is available on GitHub: <https://github.com/CH-Earth/CWARHM> (last access: 2022-07-
 778 27).

779 **Appendix A Workflow description**

780 This section describes in detail our example of a model setup workflow that follows
 781 the design principles outlined in Section 2. The workflow code, model code, software re-
 782 quirements, and data are fully open-source to follow the FAIR principles. The workflow
 783 is written in Python and Bash, using input data with global coverage, a spatially dis-
 784 tributed, physics-based hydrologic modeling framework designed to isolate individual mod-
 785 eling decisions (Clark et al., 2015a, 2015b; Clark, Zolfaghari, et al., 2021), and a network
 786 routing model (Mizukami et al., 2016, 2021) that connects the individual hydrologic model
 787 elements through a river network. This example workflow can be used to generate a ba-
 788 sic SUMMA and mizuRoute setup anywhere on the globe and is designed such that the
 789 model-agnostic parts of the code can easily feed into other modeling chains.

790 Part of the code in this repository is adapted from or inspired by work performed
 791 at the National Centre for Atmospheric Research and the University of Washington.

792 **A1 Models**

793 This section provides a brief overview of SUMMA (Clark et al., 2015a, 2015b; Clark,
 794 Zolfaghari, et al., 2021) and mizuRoute (Mizukami et al., 2016, 2021) to the extent rel-
 795 evant to understand our workflow. We refer the reader to the original papers that de-
 796 scribe each model for further details. We selected both models for their flexible nature,
 797 computational capacity to model very large domains, and availability of local expertise.
 798 Both models are written in Fortran, and their source code needs to be compiled before
 799 the models can be used.

800 ***A11 Structure for Unifying Multiple Modeling Alternatives (SUMMA)***

801 SUMMA is a process-based modeling framework designed to isolate specific mod-
 802 eling decisions and evaluate competing alternatives for each decision, with the ability to
 803 do so across multiple spatial and temporal configurations. SUMMA solves a general set
 804 of mass and energy conservation equations (Clark et al., 2015a; Clark, Zolfaghari, et al.,
 805 2021) and includes multiple alternative flux parametrizations (Clark et al., 2015b). It
 806 separates the equations that describe the model physics from the numerical methods used
 807 to solve these equations, allowing the use of state-of-the-art numerical solving techniques

(Clark, Zolfaghari, et al., 2021). SUMMA is available as Free and Open Source Software (FOSS) and under active development (see <https://www.github.com/CH-Earth/summa>).

SUMMA organizes model elements into Grouped Response Units (GRUs) that can each be further subdivided into multiple Hydrologic Response Units (HRUs). This enables flexible spatial discretization of modeling domains. For example, point-scale studies are possible by defining the domain as a single GRU that contains exactly one HRU (GRU area can be an arbitrary value because all fluxes and states are calculated per unit area; see e.g. Clark et al., 2015b). It is equally possible to mimic grid-based model setups such as commonly used in land-surface modeling schemes by defining each GRU to be equivalent to a grid cell and optionally using the HRUs to account for sub-grid variability (e.g. mimicking the tiled grid approach of traditional VIC and MESH setups; Liang et al., 1994; Pietroniro et al., 2007). Finally, GRUs can represent the (sub-)catchments of a given river system with HRUs being areas of similar hydrologic behavior within each GRU. Such model configurations can use GRUs and HRUs of irregular shape, which has several advantages over grid-based setups (see e.g. Gharari et al., 2020). Most importantly, such spatial configurations can accurately follow the actual topography of the modeling domain, and this makes model results easier to visualize and interpret. SUMMA is configured with irregularly shaped computational elements in the test cases presented in this paper.

A12 mizuRoute

mizuRoute is a vector-based river routing model specifically designed for large-domain applications such as modeling of hydrologic processes across a continental domain. It organizes the routing domain into Hydrologic Response Units (HRUs; i.e., catchments) and stream segments that meander through the HRUs and provide connections between them (Mizukami et al., 2016, 2021). It can process inputs from hydrologic models with both grid- and vector-based setups and provides different options for channel routing: Kinematic Wave Tracking (KWT) and Impulse Response Function (IRF). For a given stream segment, the IRF method constructs a set of unique Unit Hydrographs (UH) for each upstream segment which is used to route runoff from each upstream reach independently. In other words, the routed runoff in a given stream segment is a simple sum of the UH runoff generated in all upstream segments. The KWT method instead tracks channel runoff as kinematic waves moving through the stream network with their own celerity. mizuRoute is available as FOSS and under active development (see <https://github.com/ESCOMP/mizuRoute>), with a particular focus on improving its representation of lakes and reservoirs (Gharari et al., 2022; Vanderkelen et al., 2022).

A13 Note on definitions

SUMMA distinguishes between Grouped Response Units (GRUs) and Hydrological Response Units (HRUs). SUMMA's main modeling element is the GRU, which can be sub-divided into an arbitrary number of HRUs. SUMMA can handle GRUs and HRUs of any shape (e.g., points, grid cells, catchments) and these terms therefore refer to model elements of arbitrary shape and size. In this workflow, we use mizuRoute to route runoff between SUMMA's GRUs. Potentially confusingly, mizuRoute refers to all routing basins as HRUs only and does not use the term GRU. As a result, what SUMMA calls GRUs are referred to as HRUs by mizuRoute. For consistency with both sets of documentation, we use their own terminology for model elements where possible. Figure A1 shows a graphical example of the differences in terminology.

A2 Workflow description

This section briefly describes each step shown in the workflow diagram (Figure 1 in the main manuscript, with further technical details in Figures A2, A3 and A4). Fig-

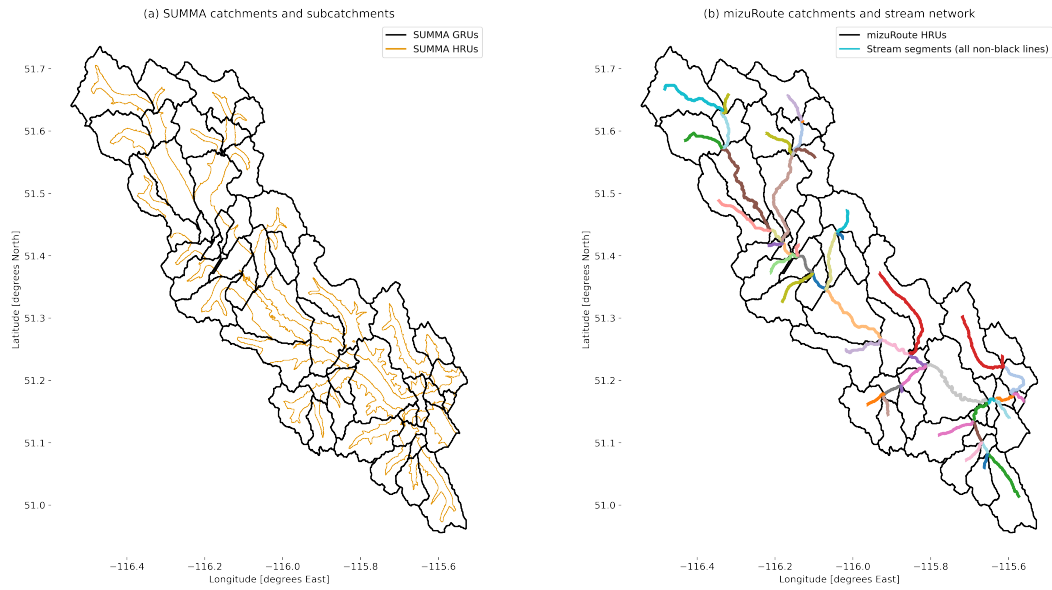


Figure A1. Catchment of the Bow River at Banff (Alberta, Canada) discretized into (a) SUMMA and (b) mizuRoute model elements, showing associated terminology. SUMMA HRUs in (a) represent different elevation bands within each SUMMA GRU. A SUMMA GRU always contains at least one SUMMA HRU. There is no upper limit to the number of HRUs a single SUMMA GRU can be divided into. A single SUMMA HRU is never part of more than one SUMMA GRU. In our example, SUMMA GRUs are identical to mizuRoute HRUs. mizuRoute stream segments are shown in different colors to emphasize that in this case each mizuRoute HRU maps 1:1 onto a single stream segment; only a single color is shown in the legend for brevity, but all non-black lines are stream segments.

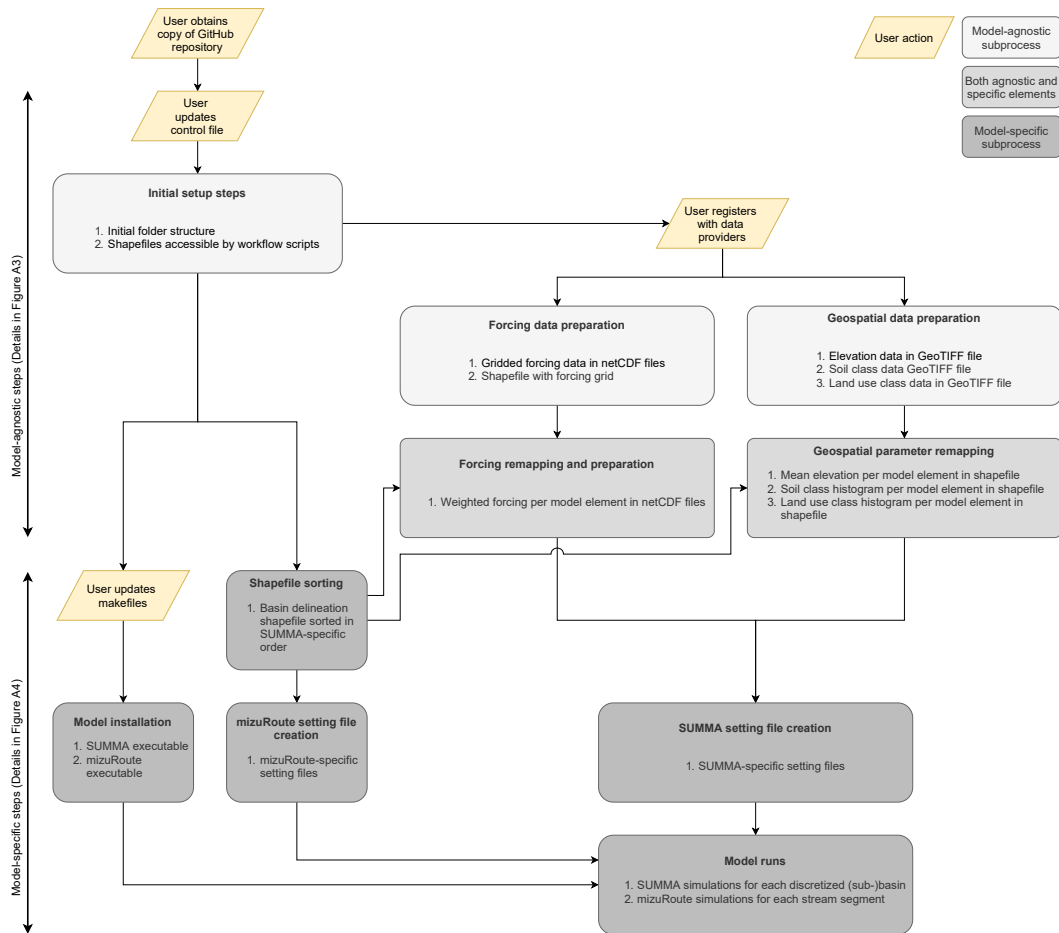


Figure A2. High-level overview of model configuration steps, using SUMMA (a process-based hydrologic model) and mizuRoute (a routing model) as example models. Configuration tasks are separated into model-agnostic and model-specific tasks (details in Figure A3 and Figure A4 respectively). Each rounded box specifies the outcomes of that configuration task as a numbered list.

857 ures are generated using the test case configured for the Bow River catchment located
 858 in Alberta, Canada (see Figure A1 for an overview of this domain). This test case covers
 859 a geographically small area (approximately 2200 km²) and uses a more complex model
 860 setup (SUMMA GRUs subdivided into multiple HRUs) than the continental test case
 861 (where SUMMA GRUs contain exactly one HRU each), making it the best choice to visualize
 862 model setup procedures. *Italicized phrases in this section indicate folders, scripts,*
 863 *or variables as found in the GitHub repository.* To start, a user would download or clone
 864 the complete GitHub repository. The following sections provide more detail about the
 865 scripts found within the GitHub repository. Although our workflow requires only limited
 866 user interaction to generate a model configuration for a new domain, we do make
 867 certain assumptions about this model configuration which users should be aware of. These
 868 assumptions are specified in each subsection.

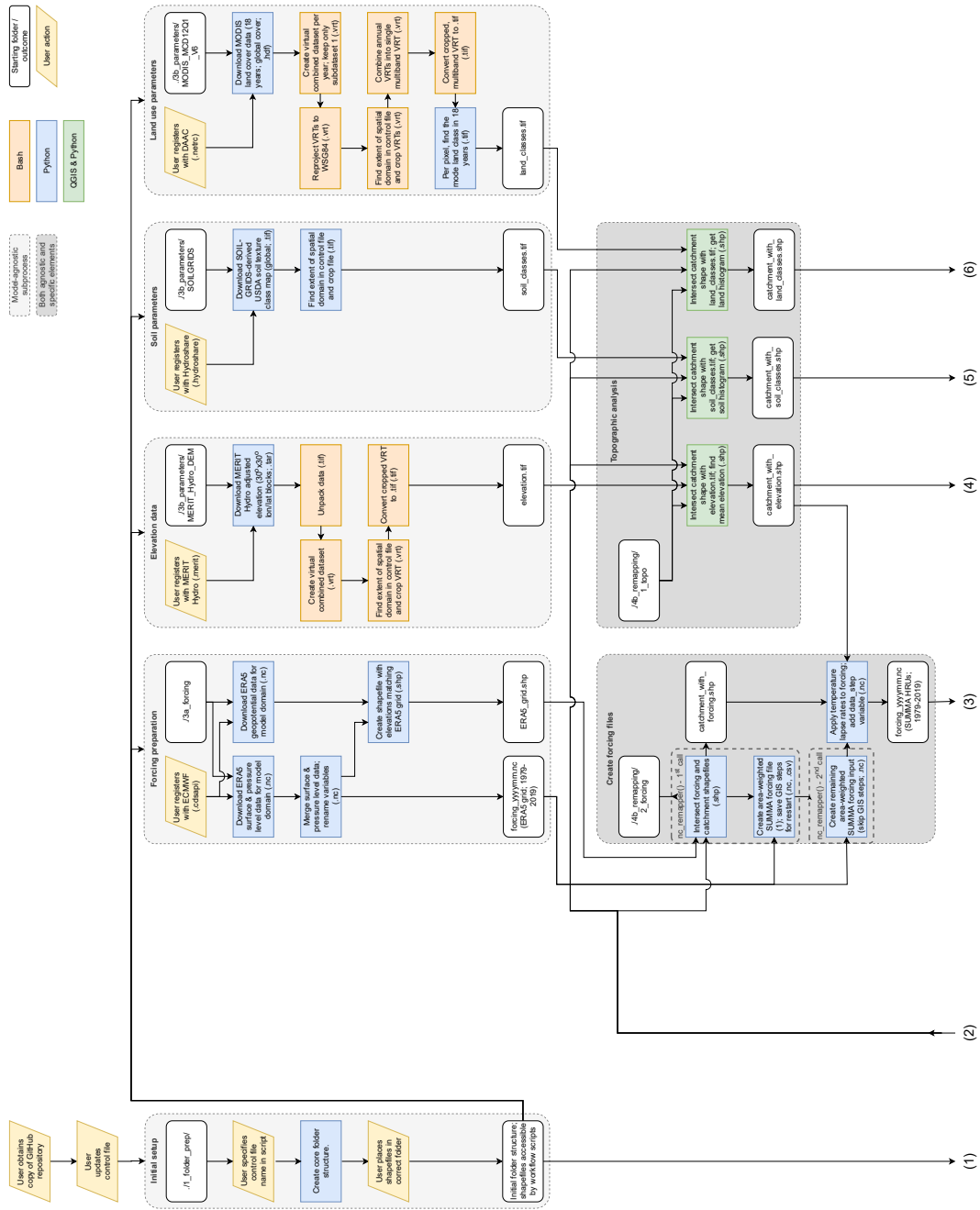


Figure A3. Model-agnostic configuration steps. Each rectangular block corresponds to a specific model setup task and is accompanied by a specific script with Python or Bash code, stored in a GitHub repository. Rounded rectangles indicate starting points of specific sub-tasks (mainly showing which folder in the repository contains certain parts of the workflow) and the outcomes of each sub-process. Parallelograms indicate actions the user must perform. Numbers show connections with the model-specific configuration tasks in Figure A4.

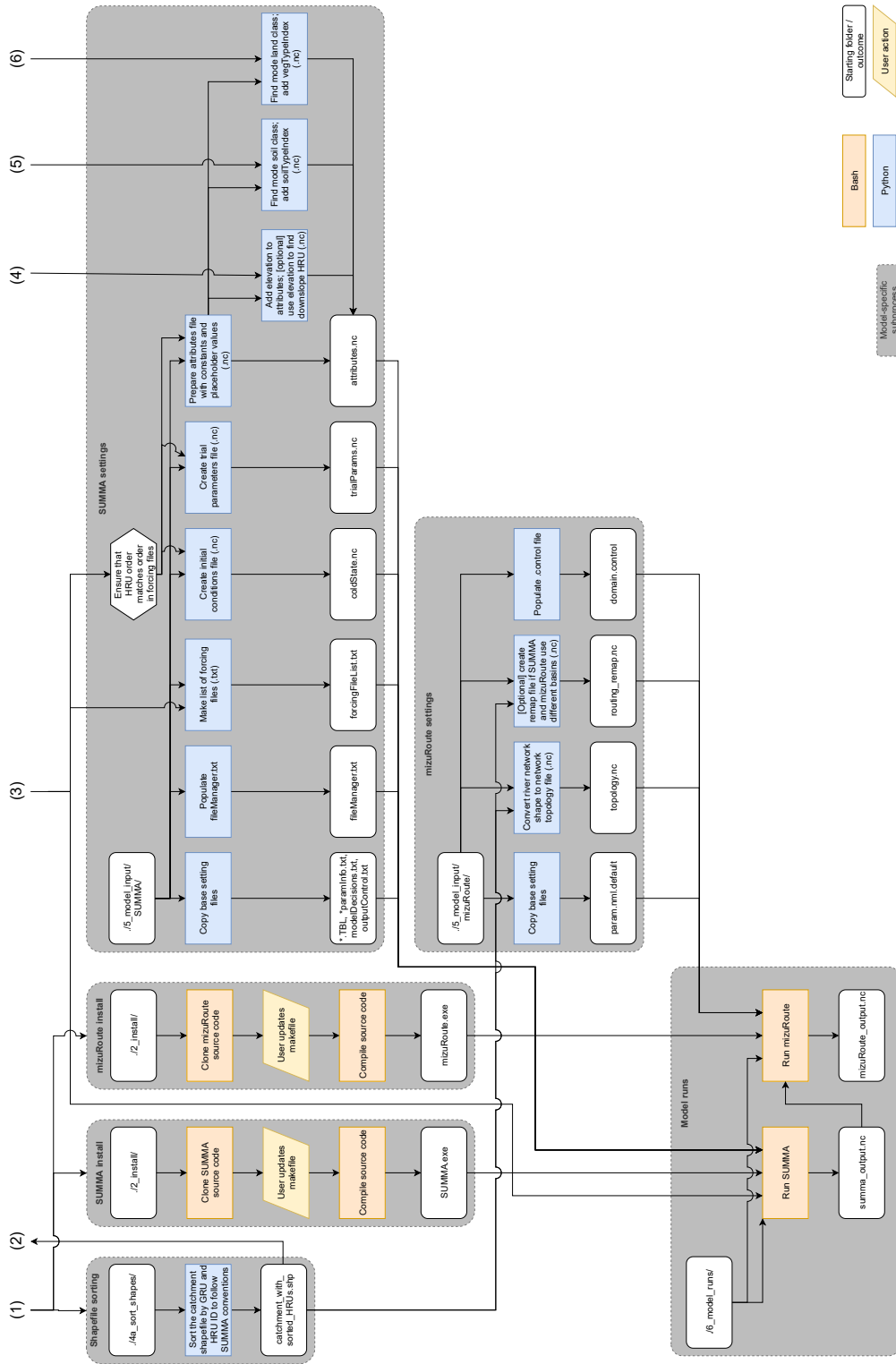


Figure A4. Model-specific configuration steps. Each rectangular block corresponds to a specific model setup task and is accompanied by a specific script with Python or Bash code, stored in a GitHub repository. Rounded rectangles indicate starting points of specific sub-tasks (mainly showing which folder in the repository contains certain parts of the workflow) and the outcomes of each sub-process. Parallelograms indicate actions the user must perform. The hexagon indicates an aspect of SUMMA’s input requirements (i.e., not an action or script) and is shown to clarify why creating the forcing files is on the critical path towards creating the other necessary model configuration files. Numbers show connections with the model-agnostic configuration tasks in Figure A3.

869 **A21 Workflow setup and folder structure**

870 This section describes the steps “User updates control file” and the steps contained
871 in the box “Initial setup” (Figure A3).

872 *A21.1 Control files* Control files are the main way for a user to interact with the
873 workflow. They contain high-level information such as file paths, file names, variable names,
874 and specification of the spatial and temporal extent of the modeling domain (see also
875 Sen Gupta et al., 2015) A new control file needs to be created by the user for each new
876 domain. As an example, the control file for the *Bow.at.Banff* test case is included as part
877 of the Github repository, in the folder `./CWARHM/0_control_files`. The READMEs of
878 each sub-folder on the GitHub repository contain a list of the settings in the control file
879 on which the scripts in that sub-folder rely.

880 *A21.2 Folder preparation* The workflow separates generated data from the code
881 used to generate the data. The script in the folder `./CWARHM/1_folder_prep` generates
882 a basic data folder structure in a location of the user’s choosing (see Figure 3b). This
883 basic folder structure generates a main data folder with a subdirectory for the current
884 domain. In this domain folder, it further generates a dedicated folder where the user can
885 place their shapefiles that delineate the SUMMA catchments (hydrologic model GRUs
886 and HRUs), mizuRoute catchments (routing model HRUs), and mizuRoute river net-
887 work. This is the only script in the workflow that needs to be manually modified if a setup
888 for a new domain is generated. A user will need to modify the variable `sourceFile` so that
889 it points to the control file for the current domain. In our example, this is set to `con-
890 trol_Bow.at.Banff.txt`. The script then copies the contents of this control file into a new
891 file called `control_active.txt`, which is the file every other workflow script will search for.
892 The variable `sourceFile` needs to be updated when a control file for a new domain is used.
893 Note that the contents of the file `control_active.txt` determine which folders and files the
894 other workflow scripts operate on.

895 *A21.3 Domain shapefiles* With a basic folder structure in place, the user can now
896 move their prepared shapefiles into the newly generated folders (assuming the control
897 file uses ‘default’ values for these shapefile paths). Briefly, the shapefiles should contain:
898 geometries that delineate the hydrologic model GRUs and HRUs, the routing model HRUs,
899 and the routing model river network in a regular latitude/longitude projection (in other
900 words, in the Coordinate Reference System defined by EPSG:4326; [https://epsg.io/
901 4326](https://epsg.io/4326) [last access, 2021-10-11]). Each shapefile needs to specify certain properties of the
902 model domain, such as identifiers for each GRU, HRU, and stream segment; HRU area
903 and centroid location, stream segment slope and length; and the stream segment ID into
904 which a given HRU drains.

905 Detailed requirements for the shapefiles are provided in the README in `./CWARHM/1_folder_prep`.
906 Example shapefiles for the *Bow.at.Banff* test case are part of the repository and can be
907 found in the subfolders of `./CWARHM/0_example`.

908 **A22 Model-agnostic workflow elements**

909 This section provides details about the model-agnostic elements of the workflow
910 (shown in light grey in Figure A3). For convenience, this section is organized to follow
911 the four model-agnostic sub processes: pre-processing of forcing, elevation, soil, and land
912 use data.

913 *A22.1 Pre-processing of forcing data* Our chosen forcing product is the ERA5
914 reanalysis data set (Copernicus Climate Change Service (C3S), 2017; Hersbach et al.,
915 2020) provided by the European Centre for Medium-Range Weather Forecasts (ECMWF).
916 ERA5 data are available as hourly data for the period 1979 to present minus 5 days, at
917 a 31 km spatial grid that covers the Earth’s surface or at a re-gridded 0.25° x 0.25° lat-

itude/longitude resolution. ERA5 data preparation includes two-way interactions between atmosphere, land surface and ocean surface components. The ERA5 model setup includes different atmospheric layers and ERA5 data are available at 137 different pressure levels (i.e., heights above the surface), as well as at the surface. The lowest atmospheric level is L137, at geopotential and geometric altitude 10 m (i.e., 10 m above the land surface). To limit the influence of ECMWF’s land model on our required forcing variables (simulating the land surface response is SUMMA’s role after all), we obtain air temperature, wind speed, and specific humidity at the lowest pressure level (Hersbach et al., 2017) instead of at the land surface. Precipitation, downward shortwave radiation, downward longwave radiation, and air pressure are unaffected by the land model coupling and can be downloaded at the surface level (Hersbach et al., 2018).

Surface and pressure level data are stored in two different data archives and are accessed in different ways. Download scripts for each separate archive are found in folder `./CWARHM/3a_forcing/1a_download_forcing`. These scripts access the C3S Climate Data Store (CDS) using the user’s credentials (instructions on how to obtain and store credentials can be found in the README in the download folder) and download the necessary data in monthly blocks of hourly data at a regular $0.25^\circ \times 0.25^\circ$ latitude/longitude resolution. The spatial and temporal extents of the domain are taken from the control file. As per the ERA5 documentation, ERA5 data should be seen as point data, even though standard visualization approaches typically show this kind of data as an interpolated grid. In our example workflow, we make the simple assumption that each ERA5 point contains forcing data that are representative for the grid of size $0.25^\circ \times 0.25^\circ$ of which the grid point is the centroid. The workflow code automatically finds which ERA5 grid points to download based on the catchment bounding box specified in the control file (Figure A5). Once downloaded, the code in `./CWARHM/3a_forcing/2_merge_forcing` can be used to merge the surface and pressure level downloads into a single netCDF file, which is used for further processing. During this merging process, the ERA5 variable names are also changed to more descriptive ones.

Gridded forcing data does not map directly onto irregular model elements such as HRUs. Code in `./CWARHM/3a_forcing/3_create_shapefile` generates a shapefile for the forcing data that outlines the forcing grid (dotted red lines in Figure A5), which is later used to find the relative contribution of each forcing grid cell to the forcing of each HRU. The elevation of each ERA5 grid point is added to this shapefile. Elevation data is later used to apply temperature lapse rates based on the difference in elevation of the ERA5 data and mean HRU elevations. As per the ERA5 documentation, the elevation of each ERA5 data point is found by dividing the geopotential [$\text{m}^2 \text{s}^{-2}$] of each point (downloaded through scripts in `./CWARHM/3a_forcing/1b_download_geopotential`) by the gravitational acceleration [m s^{-2}].

Key assumptions in this part of the workflow are (1) that the user has access to the Copernicus Data Store. Instructions on how to obtain access are given in the README in folder `./CWARHM/3a_forcing`. (2) We consider that using forcing data that are the result of interaction between the atmospheric and land surface model components is undesirable and hence somewhat limit this interaction by downloading certain variables at the lowest pressure level instead. (3) ERA5 data points are assumed to be representative of grids of size $0.25^\circ \times 0.25^\circ$. (4) Gravitational acceleration is assumed to be constant at $g = 9.80665 \text{ [m s}^{-2}\text{]}$ (Tiesinga et al., 2019), although in reality this value would vary depending on latitude and altitude. (5) ERA5 variable names are changed to more descriptive ones that are also the names SUMMA expects these variables to have.

A22.2 Pre-processing of geospatial parameter fields Three different types of geospatial data are required for our example model setup. A Digital Elevation Model (DEM) provides the elevation of each HRU and is both a SUMMA input and required to apply temperature lapse rates as a preprocessing step. Maps of soil classes and vegetation classes are needed to utilize parameter lookup tables. These tables specify values for multiple

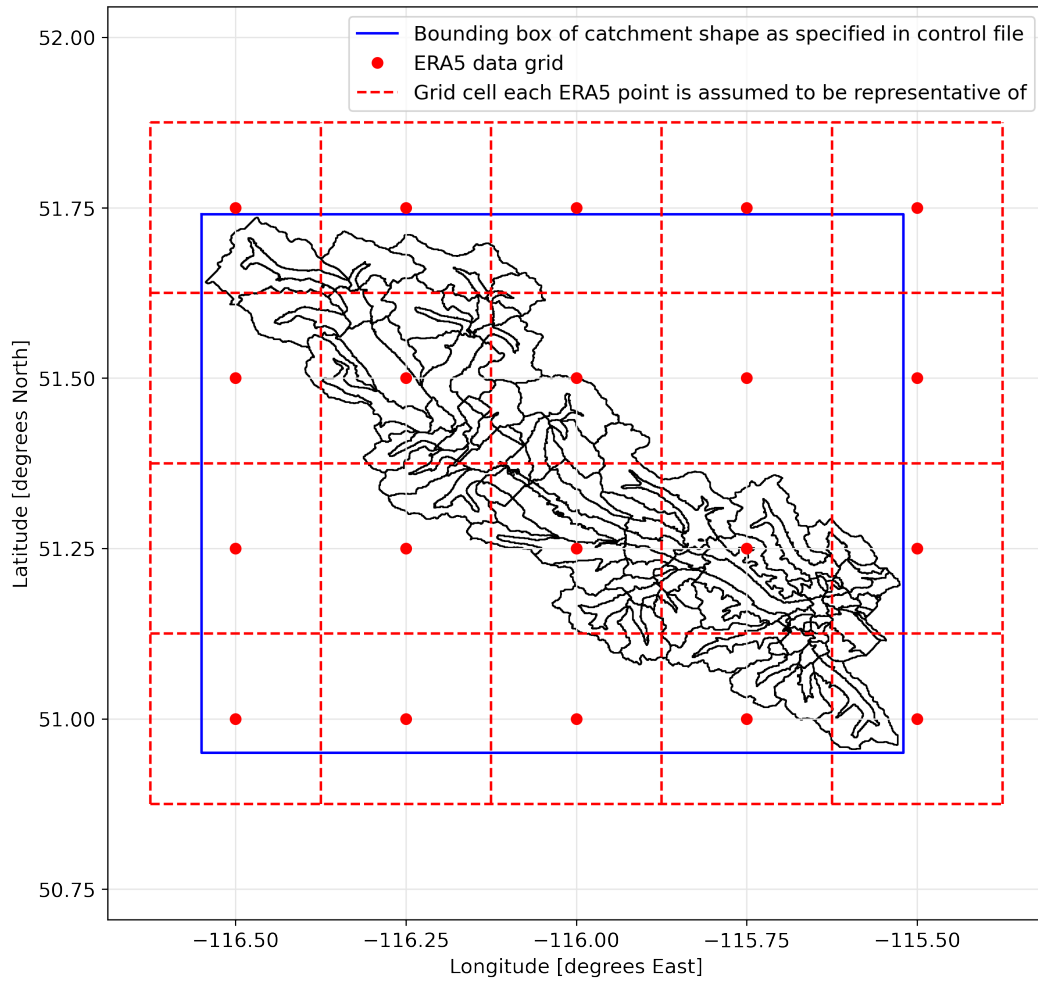


Figure A5. Overview of ERA5 data points, catchment and bounding box and how ERA5 data is assumed to overlap the catchment for the Bow at Banff test case.

971 parameters for a variety of soil and land classes. By knowing the soil or land class for
 972 a given HRU, SUMMA uses the predefined parameter values for those classes.

973 *Digital Elevation Model* We use the hydrologically adjusted elevations that are
 974 part of the MERIT Hydro dataset (Yamazaki et al., 2019) to determine HRU elevations.
 975 The MERIT Hydro hydrography maps cover the area between 90° North and 60° South
 976 at a spatial resolution of 3 arc-seconds. They are derived from the MERIT DEM (Yamazaki
 977 et al., 2017), which itself is the result of extensive error correction of the SRTM3 (Farr
 978 et al., 2007) and AW3D-30m (Tadono et al., 2016) DEMs. Scripts can be found in the
 979 subdirectories of `./CWARHM/3b_parameters/MERIT_Hydro_DEM`.

980 MERIT Hydro data are provided as compressed data packages that cover 30° x 30°
 981 areas. Based on the spatial extent of the domain, as given in the control file, the required
 982 30° areas are downloaded in compressed format. Data are then uncompressed so that
 983 the individual GeoTIFF files are accessible. These files are first combined into a Virtual
 984 Dataset (VRT), from which the exact modeling domain is extracted into a new VRT.
 985 The VRT with the extracted subdomain is then converted into a single GeoTIFF file that
 986 contains the DEM for the modeling domain. A key assumption is that the user has access
 987 to the MERIT Hydro data. Instructions on how to obtain access are given in the
 988 README in folder `./CWARHM/3b_parameters/MERIT_Hydro_DEM`.

989 *Vegetation classes* We use MODIS MCD12Q1_V6 data (Friedl and Sulla-Menashe,
 990 2019) to determine land cover classes at the HRU level. MODIS MCD12Q1 data are avail-
 991 able for the years 2001 to 2018 at a 500 m resolution. The data set contains land cover
 992 classes for multiple different land cover classification schemes. Each data layer is the re-
 993 sult of supervised classification of MODIS reflectance data (Friedl & Sulla-Menashe, 2019).
 994 Scripts can be found in the subdirectories of `./CWARHM/3b_parameters/MODIS_MCD12Q1_V6`.

995 MODIS MCD12Q1 data is provided as multiple Hierarchical Data Format (HDF)
 996 files that each cover a part of the planet’s surface at a given time. The source data files
 997 are in a sinusoidal projection and of irregular shape which makes it difficult to extract
 998 a specific region. Therefore, the workflow downloads all available individual HDF files
 999 for each year (i.e., global coverage). The individual files for each data year are combined
 1000 into one Virtual Dataset (VRT) per year for easier processing. Only the data layer of
 1001 interest, the International Geosphere Biosphere Programme (IGBP) land cover classi-
 1002 fication, is included in the VRT. The VRT is reprojected from its original sinusoidal pro-
 1003 jection into a regular latitude/longitude grid (EPSG:4326) from which the modeling do-
 1004 main is extracted. The annual VRTs are then combined into a single multi-band VRT,
 1005 which is then converted to a multi-band GeoTIFF file. The MODIS documentation ad-
 1006 vises against using the data of an individual year due to data uncertainty (Sulla-Menashe
 1007 & Friedl, 2018). Therefore, the mode land class between 2001 and 2018 is identified as
 1008 the most likely class for each pixel and stored as a new GeoTIFF file.

1009 Key assumptions are (1) that the user has access to NASA’s Earth Data website.
 1010 Instructions on how to obtain access are given in the README in folder `./CWARHM/3b_parameters/MODIS_MCD12Q1_V6`.
 1011 (2) Our example uses the IGBP land cover classification data, which is one of multiple
 1012 options available.

1013 *Soil classes* Our example uses a global map of soil texture classes (Knoben, 2021)
 1014 derived from the SoilGrids 250m dataset (Hengl et al., 2017) to specify representative
 1015 soil classes at the HRU level. The SoilGrids data are provided at a 250 m resolution and
 1016 at seven standard depths (up to 2 m depth). Data are the result of a combination of ap-
 1017 proximately 150,000 observed soil profiles, 158 remote sensing-based soil covariates, and
 1018 multiple machine learning methods. SoilGrids maps of sand, silt, and clay percentages
 1019 were converted to a soil texture map for each depth using the soil texture class bound-
 1020 aries of Benham et al. (2009). For each 250 m map point, the mode soil class of the seven
 1021 soil layers was selected as a representative value for the soil column as a whole, result-

1022 ing in a single global map of soil texture classes. The pre-processing code needed to cre-
 1023 ate this map (data download, data merge into a coherent map, conversion from percent-
 1024 ages to soil texture, finding the mode of each soil column) is accessible as part of the data
 1025 resource (Knoben, 2021). Scripts can be found in the subdirectories of `./CWARHM/3b-parameters/SOILGRIDS`.

1026 The global soil texture class map is provided at the same horizontal resolution as
 1027 the underlying SoilGrids data. The workflow first downloads a map with global cover-
 1028 age. The spatial extent of the modeling domain is extracted based on the bounding box
 1029 specified in the control file and stored as a new GeoTIFF file.

1030 Key assumptions are (1) that the user has access to Hydroshare. Instructions on
 1031 how to obtain access are given in the README in folder `./CWARHM/3b-parameters/SOILGRIDS`
 1032 and (2) the global soil map used assumes that mode soil class in each soil column can
 1033 be considered as the representative soil class for the entire soil column and that the soil
 1034 properties (such as saturated conductivity and pore volume) for the mode class are rep-
 1035 resentative of the properties of the column. This approach ignores the existence of lay-
 1036 ered soil profiles and the differences in water movement this can cause (e.g., Vanderborcht
 1037 et al., 2005). This also assumes that the most common class contains the layers that are
 1038 most hydrologically active and relevant for modeling purposes.

1039 ***A23 Mapping of data to model elements***

1040 This section provides details about the mapping of preprocessed forcing data onto
 1041 model elements (shown in the intermediate grey shade in Figure A3). This process can-
 1042 not be called truly model-agnostic because whether it is needed depends on the model
 1043 in question: some models are able to ingest the pre-processed data directly.

1044 *A23.1 Geospatial parameter fields* In our example, geospatial data in the form
 1045 of GeoTIFF files containing the DEM, land classes, and vegetation classes cannot be in-
 1046 gested by the hydrologic model directly. The data must be mapped onto the model el-
 1047 ements (HRUs) as delineated in the catchment’s shapefile. These procedures use the open-
 1048 source QGIS project (QGIS Development Team, 2021) to provide the necessary Python
 1049 functions (`./CWARHM/4b-remapping/1.topo`). Key assumptions are (1) that MERIT
 1050 Hydrologically Adjusted Elevation data need to be aggregated into mean elevation val-
 1051 ues per model element, whereas (2) soil and vegetation classes need to be aggregated into
 1052 histograms that summarize the distribution of values per model element.

1053 *A23.2 Forcing data* Figure A6 shows the original gridded air temperature val-
 1054 ues on an arbitrary day and the HRU-averaged values on that same day that are obtained
 1055 by mapping the gridded forcing data onto the model elements. For each model element,
 1056 the relative overlap with each ERA5 grid cell determines the weight with which that forc-
 1057 ing grid cell contributes to the HRU-averaged value. This procedure is applied to all seven
 1058 forcing variables and all time steps to generate HRU-averaged forcing (`./CWARHM/4b-remapping/2-forcing`).

1059 We then apply a constant environmental lapse rate of $0.0065 \text{ K}\cdot\text{m}^{-1}$ (Wallace & Hobbs,
 1060 2006, p. 421) to the HRU-averaged air temperature data to account for any differences
 1061 between ERA5 data point elevation and mean HRU elevation (Figure A7). To avoid ex-
 1062 cessive data access, the SUMMA-specific variable `data_step` (which specifies the tempo-
 1063 ral resolution of the forcing data in [s]) is added to each forcing file at the same time as
 1064 lapse rates are applied.

1065 Key assumptions are that (1) a temporally and spatially constant lapse rate can
 1066 be used. This is common in gridded analysis but typically not locally accurate (Minder
 1067 et al., 2010). Local lapse rates may be very different from this assumed value, especially
 1068 in complex terrain and at seasonal or hourly time scales (Cullen & Marshall, 2011; Min-
 1069 der et al., 2010). Regionally and temporally variable lapse rates are a possible way to
 1070 improve this part of the workflow (e.g., Dutra et al., 2020) but doing so is beyond the

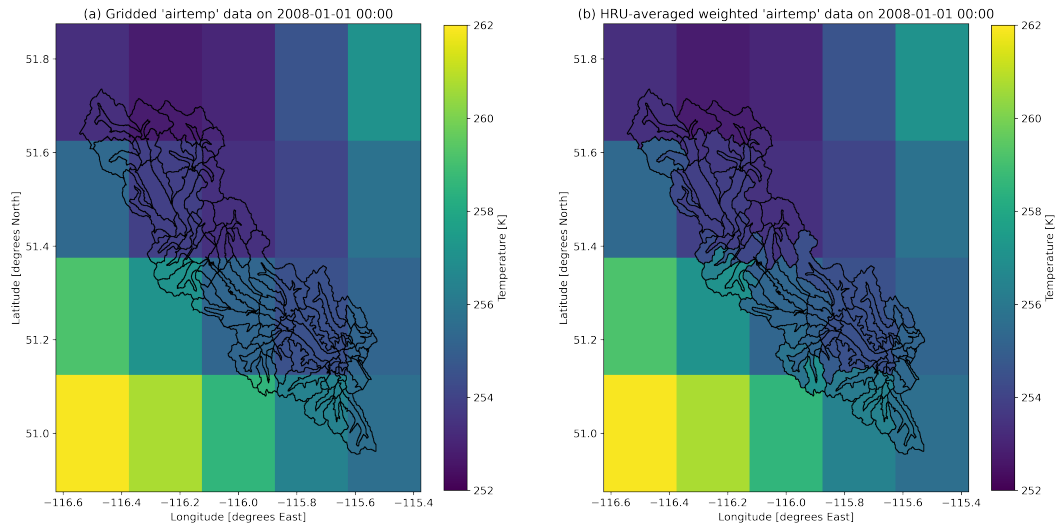


Figure A6. (a) Original gridded air temperature data as found in the ERA5 data. (b) HRU-averaged air temperature obtained as a weighted average of the relative contributions of each ERA5 grid cell to each HRU. Temperatures shown outside the catchment boundaries are the original gridded values.

1071 scope of this study. (2) The influence of slope and aspect on radiation fluxes is currently
 1072 not accounted for in forcing data preparation.

1073 *A24 Model-specific workflow elements*

1074 This section provides details model-specific steps of the workflow (shown in dark
 1075 grey in Figure 2). These steps form the interface between preprocessed data and mod-
 1076 els.

1077 *A24.1 SUMMA and mizuRoute installation* The source code for both SUMMA
 1078 and mizuRoute can be obtained through GitHub (see Section A1). Scripts in `./CWARHM/2_install`
 1079 provide code to download the latest version of both models to a local machine. Both mod-
 1080 els are written in Fortran and need to be compiled to create executables. The exact com-
 1081 mands and settings needed will vary between different computational environments. The
 1082 workflow contains examples of model compile code for a specific High Performance Com-
 1083 puting environment.

1084 Key assumptions are as follows. (1) The user has determined the appropriate set-
 1085 tings to compile both models on their own computational infrastructure and made the
 1086 necessary changes to our provided example code. (2) Both scripts assume that the “de-
 1087 velop” branch of each model is the version of interest. (3) A Linux or MacOS environ-
 1088 ment is recommended because compiling the SUMMA and mizuRoute source code re-
 1089 quires a netCDF-Fortran library to be installed locally and this library is not supported
 1090 on Windows yet. A basic alternative that avoids compiling the source code is to install
 1091 pySUMMA and mizuRoute through Conda, but this provides pre-compiled executables
 1092 only. Access to the source code is not possible and updates present on GitHub may not
 1093 immediately appear in the pySUMMA Conda distribution.

1094 *A24.2 Shapefile sorting to ensure expected order of model elements* SUMMA makes
 1095 certain assumptions about GRU and HRU order in its input files. These are: (1) GRUs
 1096 and HRUs are in the same order if the forcing files and all SUMMA input files that con-

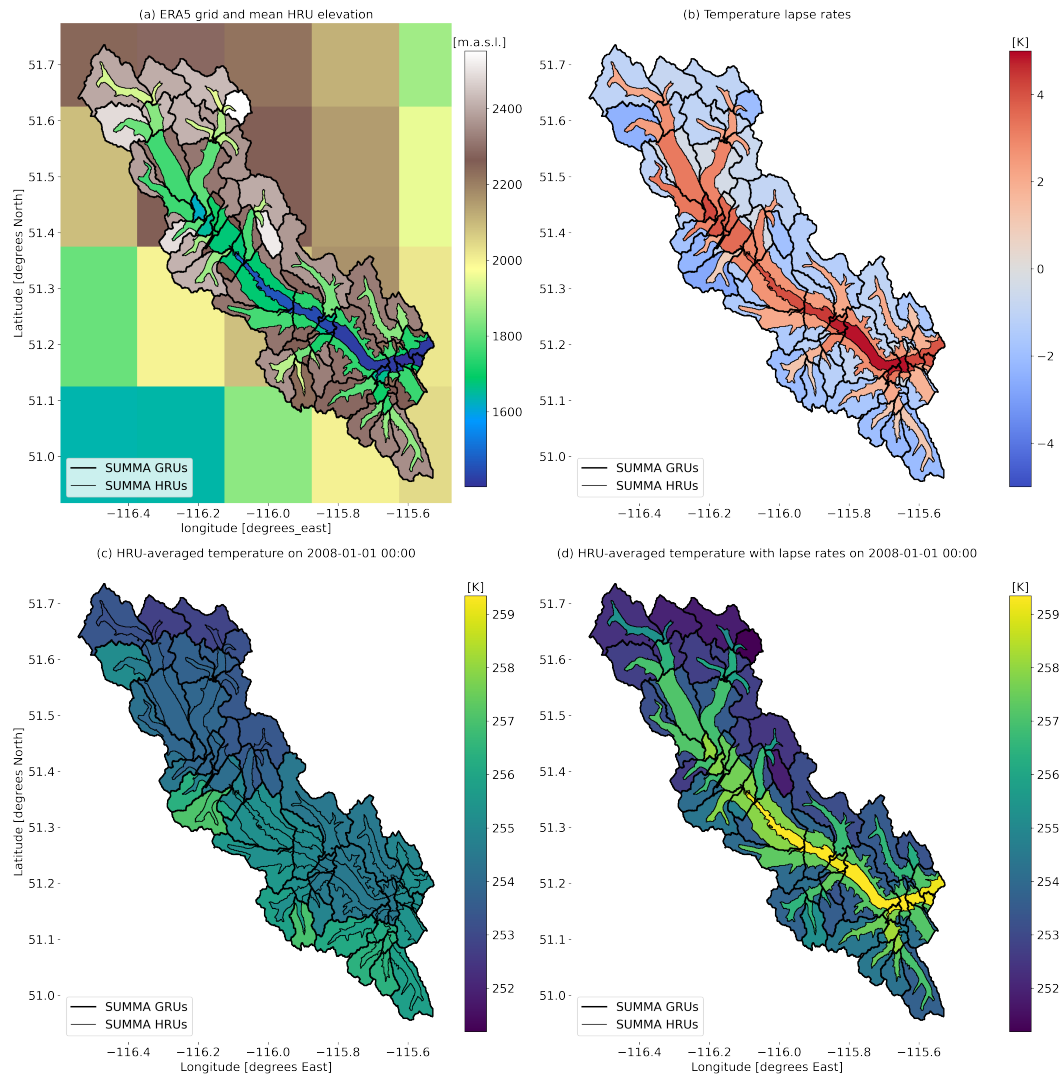


Figure A7. (a) HRU-averaged elevation derived from MERIT Hydro adjusted elevations data. ERA5 grid point elevation calculated from geopotential data and a spatially constant gravitational acceleration value, visualized as grid cells. (b) Temperature lapse values based on a constant lapse rate and a weighted difference between ERA5 grid point elevation and HRU mean elevation. (c) Air temperature data before lapse rates are applied. (d) Air temperature data after lapse rates are applied.

tain information at the GRU and HRU level; and (2) HRUs inside a given GRU are found at subsequent indices in each NetCDF file. Note that these requirements do not specify anything about the values of the GRU and HRU IDs and only focus on the order in which the IDs appear in files. The code in `./CWARHM/4a_sort_shape` sorts the shapefile that contains the catchment delineation into GRUs and HRUs before this shapefile is used by other scripts. This is more efficient than postponing this sorting until the SUMMA input files are generated. A key assumption is that computational efficiency is an important consideration and therefore this model-specific requirement should be run before the (model-agnostic) remapping is performed.

A24.3 SUMMA input files SUMMA requires several different configuration files: (1) default parameter values at the GRU and HRU level; (2) *lookup tables* with predefined soil and vegetation parameters for different soil and land classes; (3) a *model decisions* file that specifies which modeling decisions (e.g., the type of numerical solver) and flux parametrizations to use; (4) an *output control* file that specifies which internal model variables to write as model output, at which temporal resolution to do so and which, if any, summary statistics to provide; (5) a *file manager* file that specifies the file paths to all model inputs and outputs as well as the time period for the simulation; (6) a *forcing file list* file that specifies the names of all meteorological forcing files to use; (7) a *trial parameter* file that can be used to overrule any parameter value specified in the default parameter files and in the lookup tables that can be helpful to quickly test different parameter values during e.g., calibration; (8) an *initial conditions* file that specifies the model states at the beginning of the first time step; and (9) an *attribute* file that contains topographic information such as elevation, soil type, and land use type at the HRU level.

In our example setup, files with default parameter values, lookup tables, model decisions, and requested outputs are provided as part of the repository. These files do not require any information from the preprocessing steps for forcing data and geospatial parameter fields and can therefore simply be copied into the new SUMMA settings directory. The file manager and forcing file list are populated with information available in the workflow control file. The workflow generates a trial parameter file that, for our test cases, specifies a required value for only one parameter. This parameter controls the time resolution of SUMMA's simulations and is here specified as 900 seconds (i.e., four times smaller than the 1-hourly forcing data resolution) to improve numerical convergence of the model equations. The initial conditions file serves a dual purpose: it specifies the model states at the start of the simulation and the vertical discretization of the soil domain into discrete layers. In this example, SUMMA is initialized with eight soil layers of increasing thickness (0.025 m for the top layer, 1.50 m for the bottom layer), without any snow or ice present, with some soil and groundwater liquid water storage and at a constant temperature of the soil, and canopy domains of 10°C. The attributes file is populated with data from the user's shapefiles (GRU and HRU IDs, HRU-to-GRU mapping, longitude and latitude, HRU area) and from the geospatial preprocessing steps. Figure A8 shows the original geospatial parameter fields that are the outcomes of our model-agnostic preprocessing steps and how these are converted into model-specific values for SUMMA's attributes file. All scripts are available in the subdirectories of `./CWARHM/5_model_input/SUMMA`.

Key assumptions are (1) that the HRU and GRU default parameter files, model decisions and lookup table files are assumed to be sensible choices for the domain of interest. In particular, the choice of ROSETTA lookup table for soil properties (NCAR Research Applications Laboratory | RAL, 2021; U.S. Department of Agriculture: Agricultural Research Service (USDA ARS), 2021) and the modified IGBP table for vegetation properties (NCAR Research Applications Laboratory | RAL, 2021) inform how the geospatial data is preprocessed (i.e., which geospatial data sets are used and how they are transformed). (2) Vertical discretization of domain is currently set at eight soil layers with increasing thickness with depth. (3) Initial conditions are dry and warm, and there is no snow and ice present in the domain. (4) Model decisions relying on *contourLength*

1150 and *tan_slope* attributes are not supported (currently this is the baseflow model decision
 1151 *qbaseTopmodel*, as well as certain radiation calculations that account for slope inclina-
 1152 tion). Attribute variable *downHRUindex* is only used if decision *qbaseTopmodel* is ac-
 1153 tive and is therefore set to zero.

1154 *A24.4 mizuRoute input files* mizuRoute requires several configuration files: (1)
 1155 a *default parameter* file that has values for its different routing schemes; (2) a *network*
 1156 *topology* file that contains a description of the river network and its properties; (3) op-
 1157 tionally, a *remapping* file that shows how output from a hydrologic model should be mapped
 1158 onto mizuRoute’s routing network; and (4) a *mizuRoute.control* file that specifies the nec-
 1159 essary file paths and routing settings. In our example setup, a default routing param-
 1160 eter file is provided as part of the repository. This file does not require any information
 1161 from the preprocessing steps for forcing data and geospatial parameter fields and can there-
 1162 fore simply be copied into the new mizuRoute settings directory. The network topology
 1163 file contains a description of the routing basins and their associated stream segments.
 1164 It specifies which basins and segments exist, which segment each basin drains into and
 1165 physical properties of the domain such as drainage area, segment length and segment
 1166 slope. The optional remapping file only needs to be used in cases where the hydrologic
 1167 model operates on model elements that do not map directly onto mizuRoute’s routing
 1168 basins. In such a case the remapping file specifies the weight with which each hydrologic
 1169 catchment contributes flow to each routing basin. The *mizuRoute.control* file is popu-
 1170 lated with information available in the workflow control file. All scripts are available in
 1171 the subdirectories of *./CWARHM/5_model.input/mizuRoute*.

1172 Key assumptions are (1) that the provided routing parameter values are appropri-
 1173 ate for the domain and (2) Hillslope routing (i.e., routing between different SUMMA HRUs
 1174 inside a given SUMMA GRU) is performed by SUMMA. mizuRoute is configured to do
 1175 the river network routing between different SUMMA GRUs.

1176 *A24.5 Model runs* Model runs use the compiled SUMMA and mizuRoute ex-
 1177 ecutables to perform simulations using the inputs and settings defined in their respec-
 1178 tive configuration files (*./CWARHM/6_model.runs*). As part of the model run scripts,
 1179 model configuration files are copied into the simulations output directories. This ensures
 1180 traceability of the simulations by keeping a record of the settings used to generate the
 1181 simulations.

1182 ***A25 Post-processing***

1183 Post-processing of model results in this example is limited to the code needed to
 1184 generate the modeling domain figure in this manuscript (*./CWARHM/7_visualization*).
 1185 Further visualization code may be added over time, as such code is created for specific
 1186 experiments.

1187 **Appendix B Note on data accuracy**

1188 Our example workflow uses ERA5 forcing data, MERIT Hydro DEM, SOILGRIDS-
 1189 derived soil texture classes, and MODIS IGBP land classes for their global coverage. This
 1190 enables global applications of the workflow. Such global datasets are based on a com-
 1191 bination of observations and geospatial data processing methods to estimate data val-
 1192 ues for locations where no observations are available. These approaches may need to sac-
 1193 rifice local information content for global coverage and are not always able to utilize the
 1194 most accurate local data available.

1195 ERA5 is a reanalysis product from a data assimilating numerical weather predic-
 1196 tion model. ERA5 precipitation estimates compare favorably to other global products
 1197 at a daily resolution (Beck et al., 2019) but are typically not as accurate as local gauge

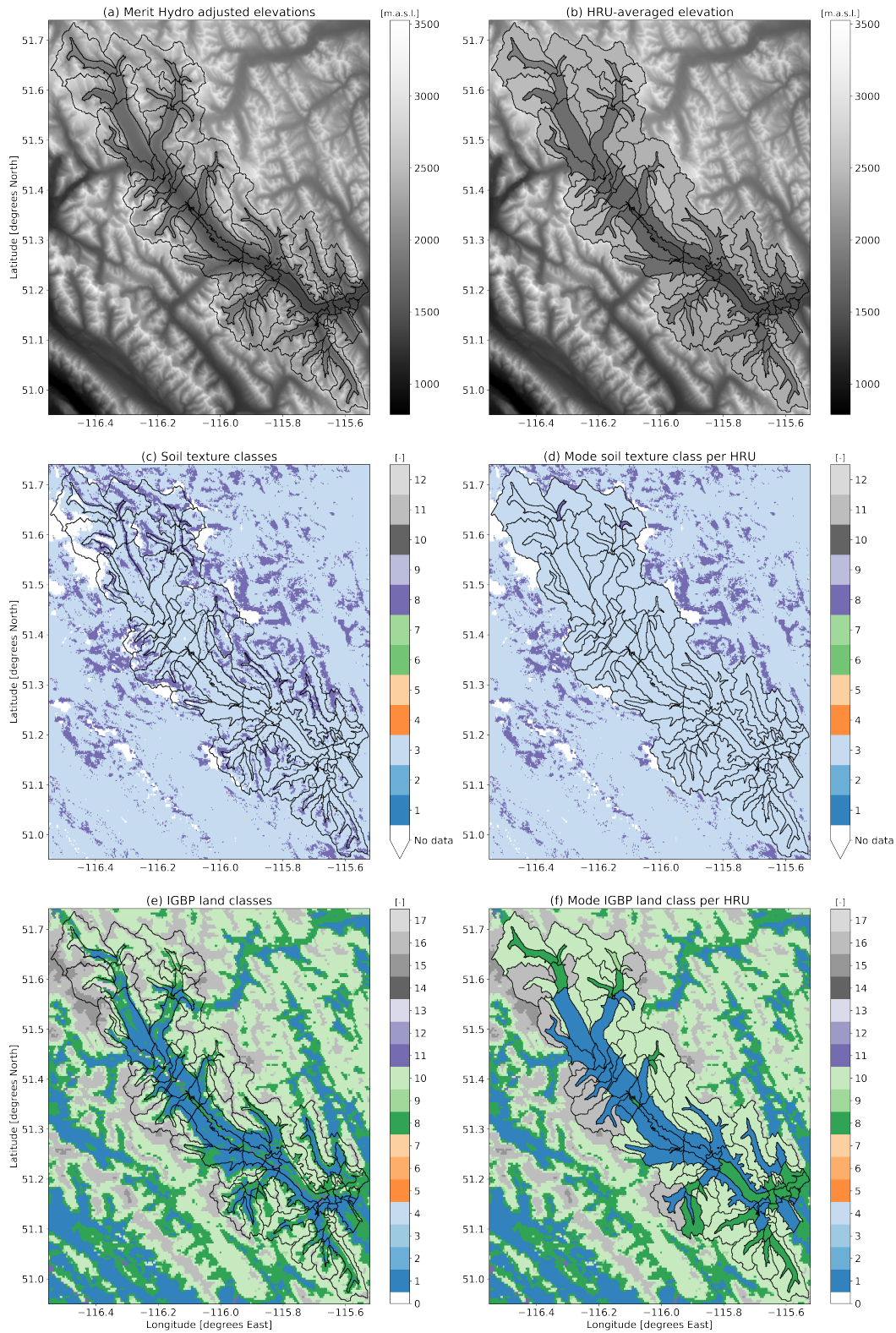


Figure A8. Mapping of geospatial parameter fields onto model elements. (a, b) MERIT Hydro adjusted elevations DEM source data and the mean elevation per HRU. (c, d) Soil texture classes derived from SOILGRIDS sand, silt and clay percentages and the most common class per HRU. (e, f) IGBP land classes from MODIS data and the most common class per HRU.

1198 or radar-based observations, especially in regions with complex topography (e.g., Am-
1199 jad et al., 2020; Q. Jiang et al., 2021; Tang et al., 2020; Xu et al., 2019). H. Jiang et al.
1200 (2020) show a similar reduced accuracy of ERA5 compared to station observations for
1201 direct and diffuse solar radiation estimates. Less is known about the accuracy of the re-
1202 maining ERA5 forcing variables used in our workflow, and it is possible that the rela-
1203 tively coarse resolution of ERA5 data means that these variables may not be as accu-
1204 rate as local products.

1205 The MERIT Hydro hydrologically adjusted elevation dataset (Yamazaki et al., 2019)
1206 is based on the MERIT DEM (Yamazaki et al., 2017), which itself is the result of ap-
1207 plying an error-removal algorithm to existing space-borne DEMs. It is available glob-
1208 ally at approximately 90 m spatial resolution. The MERIT Hydro data represent an ad-
1209 vance over earlier products such as HydroSheds (Lehner et al., 2008), especially at higher
1210 latitudes, but some uncertainty in the produced hydrography data remains in regions
1211 with low topographic variation, with endorheic basins, with seasonally varying connec-
1212 tivity, and with channel bifurcations. The MERIT Hydro hydrologically adjusted ele-
1213 vations are a modification of the MERIT DEM that satisfies the condition “downstream
1214 pixels are not higher than upstream pixels”. This procedure relies on a combination of
1215 correctly identifying endorheic basins, connections between sub-basins, and adjusting pixel
1216 elevations to create continuous flow paths. It is unknown to what extent this procedure
1217 affects the mean catchment elevation we derive from the hydrologically adjusted eleva-
1218 tion. It is plausible that mean catchment elevations derived from this data will be less
1219 accurate in regions with rapidly varying topography, where catchment slopes are steep
1220 compared to the MERIT Hydro resolution.

1221 The SoilGrids database uses observations of approximately 150,000 soil profiles, pseudo-
1222 observations that encode expert knowledge in a similar way to actual observed soil pro-
1223 files, and machine learning to provide global estimates of various soil properties at a 250
1224 m resolution. Ten-fold cross-validation of the resulting sand, silt, and clay percentage
1225 data used in our workflow shows that this approach explains approximately 75% of the
1226 variation in these soil properties. There is no systematic over or under prediction of these
1227 properties, but large differences between estimates and observations exist nonetheless
1228 in certain cases (Hengl et al., 2017).

1229 MODIS MCD12Q1_v6 data uses a combination of random forests, bias and error
1230 correction based on ancillary data, and a hidden Markov Model approach to convert pre-
1231 processed satellite reflectance imagery into land cover classification categories. Ten-fold
1232 cross-validation of the resulting classification indicates that the IGBP classes used in our
1233 workflow are accurate in approximately two-thirds of cases. Misclassifications tend to
1234 occur in regions that contain substantial land cover variability at scales smaller than the
1235 500 m MODIS resolution is provided at and along climatic gradients where the cover type
1236 changes gradually (Sulla-Menashe et al., 2019).

1237 We therefore recommend that users replace our chosen global data products with
1238 more appropriate local data if such data are available and the project scope lies within
1239 the data domain. Due to the modular nature of the workflow, this replacement requires
1240 only minimal changes to the model configuration code. In terms of Figure 7, incorpo-
1241 rating a different data set would require a new data-specific pre-processing module for
1242 which our existing workflow can serve as a guide. We emphasize that this workflow is
1243 intended to provide a baseline configuration upon which a user can improve. Our work-
1244 flow does not contain any elements that compare the resulting simulations to observa-
1245 tions to ascertain the quality of these simulations. A model setup generated through this
1246 workflow should thus not be assumed to be fit for a given purpose, unless shown to be
1247 so by the user’s own model evaluation procedures.

1248 **Open Research**

1249 The latest version of the workflow code presented in this study is available on [https://](https://github.com/CH-Earth/CWARHM)
 1250 github.com/CH-Earth/CWARHM with the specific version used to generate Figures 4, 5,
 1251 6, A1, A5-A8 via <https://dx.doi.org/10.5281/zenodo.7134868> (Knoben, Marsh, &
 1252 Tang, 2022) accessible under GNU GPL v3.0.

1253 The SUMMA (Clark et al., 2015a, 2015b; Clark, Zolfaghari, et al., 2021) versions
 1254 used for simulations in this paper can be identified by Git commit ID `edd328c8c2e7b81c3b222d4c7d2544769036fd4`
 1255 (global domain excluding North America) and Git commit ID `3d17543db618cb5b9c7600d6d0de658943056c93`
 1256 (North America domain and Bow at Banff domain). Source code accessible on [https://](https://github.com/CH-Earth/summa)
 1257 github.com/CH-Earth/summa under the GNU GPLv3 license.

1258 The mizuRoute (Mizukami et al., 2016, 2021) version used for simulations in this
 1259 paper can be identified by Git commit ID `137820620f624f84f8cdb1d4e9884b8222a3f3df`
 1260 (global domain excluding North America), Git commit ID `c2de53d242fc41b94c48119d23b78da1f35719ee`
 1261 (North America domain) and Git commit ID `d43066b56a7361f3d4a9c7b07264d7d52a9686f1`
 1262 (Bow at Banff domain). Source code accessible on <https://github.com/ESCOMP/mizuRoute>
 1263 under the GNU GPLv3 license.

1264 The single level ERA5 data (Hersbach et al., 2018) used as meteorological model
 1265 input data are available at the Copernicus Climate Change Service (C3S) Climate Data
 1266 Store (CDS) via <https://dx.doi.org/10.24381/cds.adbb2d47> under the *Licence to*
 1267 *use Copernicus Products* ([https://cds.climate.copernicus.eu/api/v2/terms/static/](https://cds.climate.copernicus.eu/api/v2/terms/static/licence-to-use-copernicus-products.pdf)
 1268 [licence-to-use-copernicus-products.pdf](https://cds.climate.copernicus.eu/api/v2/terms/static/licence-to-use-copernicus-products.pdf); last access 2021-11-04).

1269 The pressure level ERA5 data (Hersbach et al., 2017) used as meteorological model
 1270 input data are available at the Copernicus Climate Change Service (C3S) Climate Data
 1271 Store (CDS) via MARS request (no DOI) under *Licence to use Copernicus Products* ([https://](https://cds.climate.copernicus.eu/api/v2/terms/static/licence-to-use-copernicus-products.pdf)
 1272 [cds.climate.copernicus.eu/api/v2/terms/static/licence-to-use-copernicus-products](https://cds.climate.copernicus.eu/api/v2/terms/static/licence-to-use-copernicus-products.pdf)
 1273 [.pdf](https://cds.climate.copernicus.eu/api/v2/terms/static/licence-to-use-copernicus-products.pdf); last access 2021-11-04). Data downloaded on 2021-04-17 for the Bow at Banff test
 1274 case; between 2020-11-14 and 2020-12-23 for the North America test case; and on 2021-
 1275 06-20 for the global test case.

1276 The MERIT Hydro Hydrologically Adjusted Elevations (Yamazaki et al., 2019) used
 1277 as Digital Elevation Model to determine mean catchment elevations is available at [http://](http://hydro.iis.u-tokyo.ac.jp/~yamadai/MERIT_Hydro/)
 1278 hydro.iis.u-tokyo.ac.jp/~yamadai/MERIT_Hydro/ (last webpage access on 2021-11-
 1279 04) as version v1.0.1 (no DOI available; data downloaded on 2021-04-17 for the Bow at
 1280 Banff test case; on 2021-05-15 for the North America test case; between 2022-06-03 and
 1281 2022-07-02 for the global test case), accessible under CC-BY-NC 4.0 or ODbL 1.0.

1282 The MODIS MCD12Q1 V6 data (Friedl & Sulla-Menashe, 2019; Sulla-Menashe &
 1283 Friedl, 2018; Sulla-Menashe et al., 2019) used to find a representative IGBP land cover
 1284 class for each model element is available at the NASA EOSDIS Land Processes DAAC
 1285 via <https://dx.doi.org/10.5067/MODIS/MCD12Q1.006>, with no restrictions on reuse,
 1286 sale or redistribution.

1287 The Global USDA-NRCS soil texture class map (Knoben, 2021) derived from the
 1288 Soilgrids250m data set (Hengl et al., 2017) and used to find a representative USGS soil
 1289 type class for each model element is available as a Hydroshare resource via [https://dx](https://dx.doi.org/10.4211/hs.1361509511e44adfba814f6950c6e742)
 1290 [.doi.org/10.4211/hs.1361509511e44adfba814f6950c6e742](https://dx.doi.org/10.4211/hs.1361509511e44adfba814f6950c6e742), under ODbL v1.0.

1291 The shapefiles that contain the catchment delineations for all test cases are derived
 1292 from the MERIT Hydro basins data set (Lin et al., 2019), which is originally made avail-
 1293 able for research purposes on http://hydrology.princeton.edu/data/mpan/MERIT_Basins/.
 1294 The basin discretization and river network files for the Bow at Banff test case are a sub-
 1295 set of the original files, with the original basins further discretized into elevation bands.
 1296 The Bow at Banff shapefiles are provided as part of the workflow repository. For the global

1297 test case the original MERIT Hydro basin and hillslope files were merged into a single
 1298 shapefile per continent, as were the separate river network files. For the continental test
 1299 case the original MERIT Hydro basin and hillslope files were merged into a single shape-
 1300 file per continent, and updated to correct any invalid geometries in basin polygons and
 1301 to separate coastal hillslope polygons into two separate polygons if the original polygon
 1302 was intersected by a river segment. The separate river network files were merged into
 1303 a single file as well. The shapefiles that contain the catchment delineation and river net-
 1304 work for the global and continental test cases are available as a Hydroshare resource (Knoben,
 1305 Clark, et al., 2022) via <https://dx.doi.org/10.4211/hs.46d980a71d2c4365aa290dc1bfdac823>,
 1306 under CC BY-NC-SA.

1307 Acknowledgements

1308 We are thankful for the general comments for workflow improvement given by Dave
 1309 Casson, Hongli Liu, Jim Freer and Hannah Burdett. We are also thankful for the efforts
 1310 of Reza Zolfaghari and Kyle Klenk who assisted in understanding and solving specific
 1311 numerical issues, to Louise Arnal for feedback on the workflow schematics, and to Ala
 1312 Bahrami, Dayal Wijayarathne and Tricia Stadnyk for letting us share their progress on
 1313 incorporating the MESH and HYPE models into our workflow concept. Finally, we grate-
 1314 fully acknowledge the effort of the reviewers whose comments helped us clarify the mes-
 1315 sage in this paper.

1316 Wouter Knoben, Martyn Clark, Shervan Gharari, Chris Marsh, Ray Spiteri and
 1317 Guoqiang Tang were supported by the Global Water Futures program, University of Saskatchewan.
 1318 The work of David Tarboton was supported by the US National Science Foundation un-
 1319 der collaborative grants ICER 1928369 and OAC 1835569. The work of Jerad Bales was
 1320 supported by NSF grant EAR 1849458. NCAR co-author contributions were supported
 1321 by the US Army Corps of Engineers Responses to Climate Change program and the US
 1322 Bureau of Reclamation under Cooperative Agreement R16AC00039.

1323 References

- 1324 Amjad, M., Yilmaz, M. T., Yucel, I., & Yilmaz, K. K. (2020, May). Performance
 1325 evaluation of satellite- and model-based precipitation products over varying
 1326 climate and complex topography. *Journal of Hydrology*, *584*, 124707. Re-
 1327 trieved 2021-06-17, from [https://linkinghub.elsevier.com/retrieve/pii/](https://linkinghub.elsevier.com/retrieve/pii/S0022169420301670)
 1328 [S0022169420301670](https://linkinghub.elsevier.com/retrieve/pii/S0022169420301670) doi: 10.1016/j.jhydrol.2020.124707
- 1329 Archfield, S. A., Clark, M., Arheimer, B., Hay, L. E., McMillan, H., Kiang, J. E.,
 1330 ... Over, T. (2015, December). Accelerating advances in continental domain
 1331 hydrologic modeling. *Water Resources Research*, *51*(12), 10078–10091. Re-
 1332 trieved 2021-06-22, from <http://doi.wiley.com/10.1002/2015WR017498>
 1333 doi: 10.1002/2015WR017498
- 1334 Arheimer, B., Pimentel, R., Isberg, K., Crochemore, L., Andersson, J. C. M., Hasan,
 1335 A., & Pineda, L. (2020, February). Global catchment modelling using World-
 1336 Wide HYPE (WWH), open data, and stepwise parameter estimation. *Hy-*
 1337 *drology and Earth System Sciences*, *24*(2), 535–559. Retrieved 2022-06-
 1338 02, from <https://hess.copernicus.org/articles/24/535/2020/> doi:
 1339 10.5194/hess-24-535-2020
- 1340 Arsenault, R., Poulin, A., Côté, P., & Brissette, F. (2014, July). Compari-
 1341 son of Stochastic Optimization Algorithms in Hydrological Model Calibra-
 1342 tion. *Journal of Hydrologic Engineering*, *19*(7), 1374–1384. Retrieved from
 1343 [http://ascelibrary.org/doi/10.1061/\(ASCE\)HE.1943-5584.0000938](http://ascelibrary.org/doi/10.1061/(ASCE)HE.1943-5584.0000938)
 1344 (ISBN: 10.1061/(ASCE)HE.1943-5584.0000938) doi: 10.1061/(ASCE)HE.1943-
 1345 -5584.0000938
- 1346 Añel, J. A. (2017, March). Comment on “Most computational hydrology is not

- 1347 reproducible, so is it really science?” by Christopher Hutton et al.: NECES-
 1348 SARY CONDITIONS FOR REPRODUCIBILITY. *Water Resources Re-*
 1349 *search*, 53(3), 2572–2574. Retrieved 2021-02-17, from [http://doi.wiley.com/](http://doi.wiley.com/10.1002/2016WR020190)
 1350 10.1002/2016WR020190 doi: 10.1002/2016WR020190
- 1351 Bandaragoda, C., Castronova, A., Istanbuluoglu, E., Strauch, R., Nudurupati,
 1352 S., Phuong, J., ... Wang, S. (2019, October). Enabling Collaborative Nu-
 1353 merical Modeling in Earth Sciences using Knowledge Infrastructure. *Envi-*
 1354 *ronmental Modelling & Software*, 120, 104424. Retrieved 2021-06-19, from
 1355 <https://linkinghub.elsevier.com/retrieve/pii/S1364815219301562>
 1356 doi: 10.1016/j.envsoft.2019.03.020
- 1357 Barnhart, K. R., Hutton, E. W. H., Tucker, G. E., Gasparini, N. M., Istanbuluoglu,
 1358 E., Hobley, D. E. J., ... Bandaragoda, C. (2020). Short communication:
 1359 Landlab v2.0: A software package for earth surface dynamics. *Earth Surface*
 1360 *Dynamics*, 8(2), 379–397. Retrieved from [https://esurf.copernicus.org/](https://esurf.copernicus.org/articles/8/379/2020/)
 1361 articles/8/379/2020/ doi: 10.5194/esurf-8-379-2020
- 1362 Bast, R. (2019, August). A FAIRer future. *Nature Physics*, 15(8), 728–
 1363 730. Retrieved 2021-02-17, from [http://www.nature.com/articles/](http://www.nature.com/articles/s41567-019-0624-3)
 1364 s41567-019-0624-3 doi: 10.1038/s41567-019-0624-3
- 1365 Bavay, M., Reisecker, M., Egger, T., & Korhammer, D. (2022, January). In-
 1366 ishell 2.0: semantically driven automatic GUI generation for scientific mod-
 1367 els. *Geoscientific Model Development*, 15(2), 365–378. Retrieved 2022-07-
 1368 26, from <https://gmd.copernicus.org/articles/15/365/2022/> doi:
 1369 10.5194/gmd-15-365-2022
- 1370 Beck, H. E., Pan, M., Roy, T., Weedon, G. P., Pappenberger, F., van Dijk,
 1371 A. I. J. M., ... Wood, E. F. (2019, January). Daily evaluation of 26 pre-
 1372 cipitation datasets using Stage-IV gauge-radar data for the CONUS. *Hy-*
 1373 *drology and Earth System Sciences*, 23(1), 207–224. Retrieved 2021-06-
 1374 17, from <https://hess.copernicus.org/articles/23/207/2019/> doi:
 1375 10.5194/hess-23-207-2019
- 1376 Benham, E., Ahrens, R. J., & Nettleton, D. W. (2009). *MO5 Soil Technical Note-16*
 1377 *- Clarification of Textural Class Boundaries* (Tech. Rep.). Lincoln, Nebraska:
 1378 National Soil Survey Center, USDA-NRCS.
- 1379 Bennett, A., Hamman, J., & Nijssen, B. (2020, March). MetSim: A Python pack-
 1380 age for estimation and disaggregation of meteorological data. *Journal of*
 1381 *Open Source Software*, 5(47), 2042. Retrieved 2021-06-19, from [https://](https://joss.theoj.org/papers/10.21105/joss.02042)
 1382 joss.theoj.org/papers/10.21105/joss.02042 doi: 10.21105/joss.02042
- 1383 Bennett, A., Hamman, J., Nijssen, B., Clark, E., & Andreadis, K. (2018, Septem-
 1384 ber). *Uw-Hydro/Metsim: Triangular Precipitation Reference*. Zenodo.
 1385 Retrieved 2022-07-13, from <https://zenodo.org/record/1418546> doi:
 1386 10.5281/ZENODO.1418546
- 1387 Blair, G. S., Beven, K., Lamb, R., Bassett, R., Cauwenberghs, K., Hankin, B., ...
 1388 Towe, R. (2019, December). Models of everywhere revisited: A technolog-
 1389 ical perspective. *Environmental Modelling & Software*, 122, 104521. Re-
 1390 trieved 2021-06-19, from [https://linkinghub.elsevier.com/retrieve/pii/](https://linkinghub.elsevier.com/retrieve/pii/S1364815218303773)
 1391 S1364815218303773 doi: 10.1016/j.envsoft.2019.104521
- 1392 Blodgett, D., & Dornblut, I. (2018, January). *OGC® WaterML 2: Part*
 1393 *3 - Surface Hydrology Features (HY_features) - Conceptual Model*. Re-
 1394 trieved 2021-12-02, from [http://docs.opengeospatial.org/is/14-111r6/](http://docs.opengeospatial.org/is/14-111r6/14-111r6.html#_catchment_area)
 1395 14-111r6.html#_catchment_area
- 1396 Blöschl, G., Bárdossy, A., Koutsoyiannis, D., Kundzewicz, Z. W., Littlewood, I.,
 1397 Montanari, A., & Savenije, H. (2014, April). On the future of journal publi-
 1398 cations in hydrology. *Water Resources Research*, 50(4), 2795–2797. Retrieved
 1399 2021-02-17, from <http://doi.wiley.com/10.1002/2014WR015613> doi:
 1400 10.1002/2014WR015613
- 1401 Bock, a. R., Hay, L. E., McCabe, G. J., Markstrom, S. L., & Atkinson, R. D.

- 1402 (2015). Parameter regionalization of a monthly water balance model for
 1403 the conterminous United States. *Hydrology and Earth System Sciences Dis-*
 1404 *ussions*, 12(9), 10023–10066. Retrieved from <http://www.hydrol-earth>
 1405 [-syst-sci-discuss.net/12/10023/2015/hessd-12-10023-2015.html](http://www.hydrol-earth-syst-sci-discuss.net/12/10023/2015/hessd-12-10023-2015.html) doi:
 1406 10.5194/hessd-12-10023-2015
- 1407 Chaney, N., & Fisher, C. (2021, November). *chaneyn/geospatialtools: geospatial-*
 1408 *tools.nov2021*. Zenodo. Retrieved 2021-11-12, from [https://zenodo.org/](https://zenodo.org/record/5676031)
 1409 [record/5676031](https://zenodo.org/record/5676031) doi: 10.5281/ZENODO.5676031
- 1410 Choi, Y.-D. (2020). *Toward open and reproducible environmental mod-*
 1411 *eling by integrating online data repositories, computational environ-*
 1412 *ments, and model application programming interfaces*. HydroShare.
 1413 Retrieved 2020-07-13, from [http://www.hydroshare.org/resource/](http://www.hydroshare.org/resource/33cfb9622a354442b2b0a869b15ea6b0)
 1414 [33cfb9622a354442b2b0a869b15ea6b0](http://www.hydroshare.org/resource/33cfb9622a354442b2b0a869b15ea6b0)
- 1415 Choi, Y. D. (2021). *Advancing Reproducibility in Environmental Modeling: Integra-*
 1416 *tion of Open Repositories, Process Containerizations, and Seamless Workflows*
 1417 (Doctoral dissertation, University of Virginia). doi: 10.18130/G9TG-0C69
- 1418 Choi, Y.-D., Goodall, J. L., Sadler, J. M., Castronova, A. M., Bennett, A., Li, Z.,
 1419 ... Tarboton, D. G. (2021, January). Toward open and reproducible envi-
 1420 ronmental modeling by integrating online data repositories, computational
 1421 environments, and model Application Programming Interfaces. *Environ-*
 1422 *mental Modelling & Software*, 135, 104888. Retrieved 2021-01-13, from
 1423 <https://linkinghub.elsevier.com/retrieve/pii/S1364815220309452>
 1424 doi: 10.1016/j.envsoft.2020.104888
- 1425 Chuah, J., Deeds, M., Malik, T., Choi, Y., & Goodall, J. L. (2020). Documenting
 1426 Computing Environments for Reproducible Experiments. In *Parallel Comput-*
 1427 *ing: Technology Trends* (Edited by I. Foster, G. R. Joubert, L. Kučera, W. E.
 1428 Nagel and F. Peters ed., Vol. 36, pp. 756–765). Amsterdam, Netherlands: IOS
 1429 Press. Retrieved from <http://doi.org/10.3233/APC200106>
- 1430 Clark, M. P., Luce, C. H., AghaKouchak, A., Berghuijs, W., David, C. H., Duan,
 1431 Q., ... Tyler, S. W. (2021, April). Open Science: Open Data, Open Models,
 1432 ... and Open Publications? *Water Resources Research*, 57(4). Retrieved 2021-
 1433 11-01, from <https://onlinelibrary.wiley.com/doi/10.1029/2020WR029480>
 1434 doi: 10.1029/2020WR029480
- 1435 Clark, M. P., Nijssen, B., Lundquist, J. D., Kavetski, D., Rupp, D. E., Woods,
 1436 R. A., ... Rasmussen, R. M. (2015a, April). A unified approach for process-
 1437 based hydrologic modeling: 1. Modeling concept. *Water Resources Research*,
 1438 51(4), 2498–2514. Retrieved 2021-02-03, from [https://onlinelibrary.wiley](https://onlinelibrary.wiley.com/doi/abs/10.1002/2015WR017198)
 1439 [.com/doi/abs/10.1002/2015WR017198](https://onlinelibrary.wiley.com/doi/abs/10.1002/2015WR017198) doi: 10.1002/2015WR017198
- 1440 Clark, M. P., Nijssen, B., Lundquist, J. D., Kavetski, D., Rupp, D. E., Woods,
 1441 R. A., ... Marks, D. G. (2015b, April). A unified approach for process-
 1442 based hydrologic modeling: 2. Model implementation and case studies.
 1443 *Water Resources Research*, 51(4), 2515–2542. Retrieved 2021-02-03, from
 1444 <https://onlinelibrary.wiley.com/doi/abs/10.1002/2015WR017200> doi:
 1445 10.1002/2015WR017200
- 1446 Clark, M. P., Vogel, R. M., Lamontagne, J. R., Mizukami, N., Knoben, W. J. M.,
 1447 Tang, G., ... Papalexiou, S. M. (2021, September). The Abuse of Popular
 1448 Performance Metrics in Hydrologic Modeling. *Water Resources Research*,
 1449 57(9). Retrieved 2021-11-24, from [https://onlinelibrary.wiley.com/doi/](https://onlinelibrary.wiley.com/doi/10.1029/2020WR029001)
 1450 [10.1029/2020WR029001](https://onlinelibrary.wiley.com/doi/10.1029/2020WR029001) doi: 10.1029/2020WR029001
- 1451 Clark, M. P., Zolfaghari, R., Green, K. R., Trim, S., Knoben, W. J. M., Bennett,
 1452 A., ... Spiteri, R. J. (2021, April). The numerical implementation of
 1453 land models: Problem formulation and laugh tests. *Journal of Hydrome-*
 1454 *teorology*. Retrieved 2021-04-20, from [https://journals.ametsoc.org/](https://journals.ametsoc.org/view/journals/hydr/aop/JHM-D-20-0175.1/JHM-D-20-0175.1.xml)
 1455 [view/journals/hydr/aop/JHM-D-20-0175.1/JHM-D-20-0175.1.xml](https://journals/hydr/aop/JHM-D-20-0175.1/JHM-D-20-0175.1.xml) doi:
 1456 10.1175/JHM-D-20-0175.1

- 1457 Coon, E. T., & Shuai, P. (2022, November). Watershed Workflow: A toolset
1458 for parameterizing data-intensive, integrated hydrologic models. *Environ-*
1459 *mental Modelling & Software*, *157*, 105502. Retrieved 2022-10-05, from
1460 <https://linkinghub.elsevier.com/retrieve/pii/S1364815222002031>
1461 doi: 10.1016/j.envsoft.2022.105502
- 1462 Copernicus Climate Change Service (C3S). (2017). *ERA5: Fifth generation of*
1463 *ECMWF atmospheric reanalyses of the global climate*. Retrieved 2020-03-26,
1464 from <https://cds.climate.copernicus.eu/cdsapp#!/home>
- 1465 Cullen, R. M., & Marshall, S. J. (2011, September). Mesoscale Temperature
1466 Patterns in the Rocky Mountains and Foothills Region of Southern Al-
1467 berta. *Atmosphere-Ocean*, *49*(3), 189–205. Retrieved 2021-03-17, from
1468 <http://www.tandfonline.com/doi/abs/10.1080/07055900.2011.592130>
1469 doi: 10.1080/07055900.2011.592130
- 1470 Dash, P., & Tarboton, D. (2022). *Hydro-DS*. Retrieved 2022-07-13, from [https://](https://github.com/CI-WATER/Hydro-DS/)
1471 github.com/CI-WATER/Hydro-DS/
- 1472 Doherty, J., & Skahill, B. E. (2006, August). An advanced regularization method-
1473 ology for use in watershed model calibration. *Journal of Hydrology*, *327*(3-4),
1474 564–577. Retrieved 2022-07-28, from [https://linkinghub.elsevier.com/](https://linkinghub.elsevier.com/retrieve/pii/S0022169405006542)
1475 [retrieve/pii/S0022169405006542](https://linkinghub.elsevier.com/retrieve/pii/S0022169405006542) doi: 10.1016/j.jhydrol.2005.11.058
- 1476 Dutra, E., Muñoz-Sabater, J., Bousssetta, S., Komori, T., Hirahara, S., & Balsamo,
1477 G. (2020, May). Environmental Lapse Rate for High-Resolution Land Sur-
1478 face Downscaling: An Application to ERA5. *Earth and Space Science*, *7*(5).
1479 Retrieved 2021-03-17, from [https://onlinelibrary.wiley.com/doi/abs/](https://onlinelibrary.wiley.com/doi/abs/10.1029/2019EA000984)
1480 [10.1029/2019EA000984](https://onlinelibrary.wiley.com/doi/abs/10.1029/2019EA000984) doi: 10.1029/2019EA000984
- 1481 Essawy, B. T., Goodall, J. L., Voce, D., Morsy, M. M., Sadler, J. M., Choi, Y. D.,
1482 ... Malik, T. (2020, December). A taxonomy for reproducible and replicable
1483 research in environmental modelling. *Environmental Modelling & Software*,
1484 *134*, 104753. Retrieved 2021-06-19, from [https://linkinghub.elsevier](https://linkinghub.elsevier.com/retrieve/pii/S1364815219311612)
1485 [.com/retrieve/pii/S1364815219311612](https://linkinghub.elsevier.com/retrieve/pii/S1364815219311612) doi: 10.1016/j.envsoft.2020.104753
- 1486 Essawy, B. T., Goodall, J. L., Xu, H., Rajasekar, A., Myers, J. D., Kugler, T. A.,
1487 ... Moore, R. W. (2016, April). Server-side workflow execution using data
1488 grid technology for reproducible analyses of data-intensive hydrologic sys-
1489 tems. *Earth and Space Science*, *3*(4), 163–175. Retrieved 2021-11-23, from
1490 <https://onlinelibrary.wiley.com/doi/10.1002/2015EA000139> doi:
1491 [10.1002/2015EA000139](https://onlinelibrary.wiley.com/doi/10.1002/2015EA000139)
- 1492 Famiglietti, J. S., Murdoch, L., Lakshmi, V., Arrigo, J., & Hooper, R. (2011). *Es-*
1493 *tablishing a Framework for Community Modeling in Hydrologic Science* (Tech.
1494 Rep.). Beckman Center of the National Academies, University of California at
1495 Irvine.
- 1496 Farr, T. G., Rosen, P. A., Caro, E., Crippen, R., Duren, R., Hensley, S., ... Alsdorf,
1497 D. (2007, May). The Shuttle Radar Topography Mission. *Reviews of Geo-*
1498 *physics*, *45*(2), RG2004. Retrieved 2021-06-12, from [http://doi.wiley.com/](http://doi.wiley.com/10.1029/2005RG000183)
1499 [10.1029/2005RG000183](http://doi.wiley.com/10.1029/2005RG000183) doi: 10.1029/2005RG000183
- 1500 Flügel, W.-A. (1995, April). Delineating hydrological response units by ge-
1501 ographical information system analyses for regional hydrological mod-
1502 elling using PRMS/MMS in the drainage basin of the River Bröl, Ger-
1503 many. *Hydrological Processes*, *9*(3-4), 423–436. Retrieved 2022-07-26, from
1504 <https://onlinelibrary.wiley.com/doi/10.1002/hyp.3360090313> doi:
1505 [10.1002/hyp.3360090313](https://onlinelibrary.wiley.com/doi/10.1002/hyp.3360090313)
- 1506 Friedl, M., & Sulla-Menashe, D. (2019). *MCD12Q1 MODIS/Terra+Aqua Land*
1507 *Cover Type Yearly L3 Global 500m SIN Grid V006*. NASA EOSDIS Land
1508 Processes DAAC. Retrieved 2021-06-12, from [https://lpdaac.usgs.gov/](https://lpdaac.usgs.gov/products/mcd12q1v006/)
1509 [products/mcd12q1v006/](https://lpdaac.usgs.gov/products/mcd12q1v006/) (Type: dataset) doi: 10.5067/MODIS/
1510 [MCD12Q1.006](https://lpdaac.usgs.gov/products/mcd12q1v006/)
- 1511 Gan, T., Tarboton, D. G., Dash, P., Gichamo, T. Z., & Horsburgh, J. S. (2020,

- 1512 August). Integrating hydrologic modeling web services with online data
 1513 sharing to prepare, store, and execute hydrologic models. *Environmental*
 1514 *Modelling & Software*, *130*, 104731. Retrieved 2021-06-19, from
 1515 <https://linkinghub.elsevier.com/retrieve/pii/S1364815219311661>
 1516 doi: 10.1016/j.envsoft.2020.104731
- 1517 Gharari, S., Clark, M. P., Mizukami, N., Knoben, W. J. M., Wong, J. S., &
 1518 Pietroniro, A. (2020). Flexible vector-based spatial configurations in
 1519 land models. *Hydrology and Earth System Sciences*, *24*, 5953–5971. doi:
 1520 <https://doi.org/10.5194/hess-24-5953-2020>
- 1521 Gharari, S., Vanderkelen, I., Tefs, A., Mizukami, N., Stadnyk, T. A., Lawrence, D.,
 1522 & Clark, M. P. (2022, March). *A Flexible Multi-Scale Framework to Simulate*
 1523 *Lakes and Reservoirs in Earth System Models* (preprint). Hydrology. Retrieved
 1524 2022-07-25, from <http://www.essoar.org/doi/10.1002/essoar.10510902.1>
 1525 doi: 10.1002/essoar.10510902.1
- 1526 Gichamo, T. Z., Sazib, N. S., Tarboton, D. G., & Dash, P. (2020, March). HydroDS:
 1527 Data services in support of physically based, distributed hydrological models.
 1528 *Environmental Modelling & Software*, *125*, 104623. Retrieved 2021-06-19, from
 1529 <https://linkinghub.elsevier.com/retrieve/pii/S1364815217308009>
 1530 doi: 10.1016/j.envsoft.2020.104623
- 1531 Gil, Y., David, C. H., Demir, I., Essawy, B. T., Fulweiler, R. W., Goodall, J. L.,
 1532 ... Yu, X. (2016, October). Toward the Geoscience Paper of the Future:
 1533 Best practices for documenting and sharing research from data to software to
 1534 provenance. *Earth and Space Science*, *3*(10), 388–415. Retrieved 2021-11-24,
 1535 from <https://onlinelibrary.wiley.com/doi/10.1002/2015EA000136> doi:
 1536 10.1002/2015EA000136
- 1537 Gupta, H. V., Wagener, T., & Liu, Y. (2008). Reconciling theory with observations :
 1538 elements of a diagnostic approach to model evaluation. *Hydrological Processes*,
 1539 *3813*(22), 3802–3813. doi: <https://doi.org/10.1002/hyp.6989>
- 1540 Hamman, J. J., Nijssen, B., Bohn, T. J., Gergel, D. R., & Mao, Y. (2018, Au-
 1541 gust). The Variable Infiltration Capacity model version 5 (VIC-5): in-
 1542 frastructure improvements for new applications and reproducibility. *Geo-*
 1543 *scientific Model Development*, *11*(8), 3481–3496. Retrieved 2021-04-30,
 1544 from <https://gmd.copernicus.org/articles/11/3481/2018/> doi:
 1545 10.5194/gmd-11-3481-2018
- 1546 Havens, S., Marks, D., Sandusky, M., Hedrick, A., Johnson, M., Robertson, M., &
 1547 Trujillo, E. (2020, November). Automated Water Supply Model (AWSM):
 1548 Streamlining and standardizing application of a physically based snow model
 1549 for water resources and reproducible science. *Computers & Geosciences*, *144*,
 1550 104571. Retrieved 2021-11-10, from [https://linkinghub.elsevier.com/](https://linkinghub.elsevier.com/retrieve/pii/S0098300420305598)
 1551 [retrieve/pii/S0098300420305598](https://linkinghub.elsevier.com/retrieve/pii/S0098300420305598) doi: 10.1016/j.cageo.2020.104571
- 1552 Havens, S., Marks, D., Sandusky, M., Johnson, M., Robertson, M., Hedrick, A., &
 1553 Kormos, P. (2019, September). *Automated Water Supply Model (AWSM)*.
 1554 Zenodo. Retrieved 2022-07-13, from <https://zenodo.org/record/3455762>
 1555 doi: 10.5281/ZENODO.3455762
- 1556 Hengl, T., Mendes de Jesus, J., Heuvelink, G. B. M., Ruiperez Gonzalez, M.,
 1557 Kilibarda, M., Blagotić, A., ... Kempen, B. (2017, February). SoilGrids250m:
 1558 Global gridded soil information based on machine learning. *PLOS ONE*,
 1559 *12*(2), e0169748. Retrieved 2021-06-11, from [https://dx.plos.org/10.1371/](https://dx.plos.org/10.1371/journal.pone.0169748)
 1560 [journal.pone.0169748](https://dx.plos.org/10.1371/journal.pone.0169748) doi: 10.1371/journal.pone.0169748
- 1561 Hersbach, H., Bell, B., Berrisford, P., Biavati, G., Horányi, A., Muñoz Sabater, J.,
 1562 ... Thépaut, J.-N. (2018). *ERA5 hourly data on single levels from 1979 to*
 1563 *present*. doi: 10.24381/cds.adbb2d47
- 1564 Hersbach, H., Bell, B., Berrisford, P., Hirahara, S., Horányi, A., Muñoz-Sabater, J.,
 1565 ... Thépaut, J.-N. (2017). *Complete ERA5: Fifth generation of ECMWF*
 1566 *atmospheric reanalyses of the global climate*.

- 1567 Hersbach, H., Bell, B., Berrisford, P., Hirahara, S., Horányi, A., Muñoz-Sabater, J.,
 1568 ... Thépaut, J. (2020, July). The ERA5 global reanalysis. *Quarterly Journal*
 1569 *of the Royal Meteorological Society*, 146(730), 1999–2049. Retrieved 2021-11-
 1570 23, from <https://onlineibrary.wiley.com/doi/10.1002/qj.3803> doi:
 1571 10.1002/qj.3803
- 1572 Hobley, D. E. J., Adams, J. M., Nudurupati, S. S., Hutton, E. W. H., Gasparini,
 1573 N. M., Istanbuluoglu, E., & Tucker, G. E. (2017). Creative computing
 1574 with landlab: an open-source toolkit for building, coupling, and exploring
 1575 two-dimensional numerical models of earth-surface dynamics. *Earth Surface*
 1576 *Dynamics*, 5(1), 21–46. doi: 10.5194/esurf-5-21-2017
- 1577 Husain, S. Z., Alavi, N., Bélair, S., Carrera, M., Zhang, S., Fortin, V., ... Gau-
 1578 thier, N. (2016, August). The Multibudget Soil, Vegetation, and Snow (SVS)
 1579 Scheme for Land Surface Parameterization: Offline Warm Season Evalua-
 1580 tion. *Journal of Hydrometeorology*, 17(8), 2293–2313. Retrieved 2021-11-24,
 1581 from <http://journals.ametsoc.org/doi/10.1175/JHM-D-15-0228.1> doi:
 1582 10.1175/JHM-D-15-0228.1
- 1583 Hut, R. W., van de Giesen, N. C., & Drost, N. (2017, May). Comment on “Most
 1584 computational hydrology is not reproducible, so is it really science?” by
 1585 Christopher Hutton et al.: Let hydrologists learn the latest computer sci-
 1586 ence by working with Research Software Engineers (RSEs) and not reinvent
 1587 the waterwheel ourselves. *Water Resources Research*, 53(5), 4524–4526. Re-
 1588 trieved 2021-02-17, from <http://doi.wiley.com/10.1002/2017WR020665> doi:
 1589 10.1002/2017WR020665
- 1590 Hutton, C., Wagener, T., Freer, J., Han, D., Duffy, C., & Arheimer, B. (2016,
 1591 October). Most computational hydrology is not reproducible, so is it really
 1592 science?: REPRODUCIBLE COMPUTATIONAL HYDROLOGY. *Water*
 1593 *Resources Research*, 52(10), 7548–7555. Retrieved 2021-02-17, from [http://](http://doi.wiley.com/10.1002/2016WR019285)
 1594 doi.wiley.com/10.1002/2016WR019285 doi: 10.1002/2016WR019285
- 1595 Jiang, H., Yang, Y., Bai, Y., & Wang, H. (2020, January). Evaluation of the To-
 1596 tal, Direct, and Diffuse Solar Radiations From the ERA5 Reanalysis Data in
 1597 China. *IEEE Geoscience and Remote Sensing Letters*, 17(1), 47–51. Retrieved
 1598 2021-06-17, from <https://ieeexplore.ieee.org/document/8725564/> doi:
 1599 10.1109/LGRS.2019.2916410
- 1600 Jiang, Q., Li, W., Fan, Z., He, X., Sun, W., Chen, S., ... Wang, J. (2021, April).
 1601 Evaluation of the ERA5 reanalysis precipitation dataset over Chinese Main-
 1602 land. *Journal of Hydrology*, 595, 125660. Retrieved 2021-06-17, from
 1603 <https://linkinghub.elsevier.com/retrieve/pii/S0022169420311215>
 1604 doi: 10.1016/j.jhydrol.2020.125660
- 1605 Knoben, W. J. M. (2021). *Global USDA-NRCS soil texture class map* (Tech.
 1606 Rep.). Retrieved 2021-06-11, from [http://www.hydroshare.org/resource/](http://www.hydroshare.org/resource/1361509511e44adfb814f6950c6e742)
 1607 [1361509511e44adfb814f6950c6e742](http://www.hydroshare.org/resource/1361509511e44adfb814f6950c6e742) (Type: dataset) doi: 10.4211/
 1608 [hs.1361509511e44adfb814f6950c6e742](http://www.hydroshare.org/resource/1361509511e44adfb814f6950c6e742)
- 1609 Knoben, W. J. M., Clark, M. P., Gharari, S., & Tang, G. (2022). *Community*
 1610 *Workflows to Advance Reproducibility in Hydrologic Modeling: Separating*
 1611 *model-agnostic and model-specific configuration steps in applications of large-*
 1612 *domain hydrologic models - Continental basin discretizations and river net-*
 1613 *works* (Tech. Rep.). Retrieved 2022-07-28, from [http://www.hydroshare.org/](http://www.hydroshare.org/resource/46d980a71d2c4365aa290dc1bfdac823)
 1614 [resource/46d980a71d2c4365aa290dc1bfdac823](http://www.hydroshare.org/resource/46d980a71d2c4365aa290dc1bfdac823) (Type: dataset) doi:
 1615 10.4211/hs.46d980a71d2c4365aa290dc1bfdac823
- 1616 Knoben, W. J. M., Marsh, C. B., & Tang, G. (2022, October). *CH-*
 1617 *Earth/CWARHM: CWARM workflow updates during peer review*. Zenodo.
 1618 Retrieved 2022-10-02, from <https://zenodo.org/record/7134868> doi:
 1619 10.5281/ZENODO.7134868
- 1620 Kurtzer, G. M., Cclerget, Bauer, M., Kaneshiro, I., Trudgian, D., & Godlove,
 1621 D. (2021, April). *hpcng/singularity: Singularity 3.7.3*. Zenodo. Re-

- 1622 trieved 2022-07-13, from <https://zenodo.org/record/1310023> doi:
1623 10.5281/ZENODO.1310023
- 1624 Kurtzer, G. M., Sochat, V., & Bauer, M. W. (2017, May). Singularity: Scientific
1625 containers for mobility of compute. *PLOS ONE*, *12*(5), e0177459. Retrieved
1626 2021-11-11, from <https://dx.plos.org/10.1371/journal.pone.0177459>
1627 doi: 10.1371/journal.pone.0177459
- 1628 Lehner, B., & Grill, G. (2013, July). Global river hydrography and network
1629 routing: baseline data and new approaches to study the world's large river
1630 systems: GLOBAL RIVER HYDROGRAPHY AND NETWORK ROUT-
1631 ING. *Hydrological Processes*, *27*(15), 2171–2186. Retrieved 2021-11-10,
1632 from <https://onlinelibrary.wiley.com/doi/10.1002/hyp.9740> doi:
1633 10.1002/hyp.9740
- 1634 Lehner, B., Verdin, K., & Jarvis, A. (2008). New Global Hydrography Derived From
1635 Spaceborne Elevation Data. *Eos, Transactions American Geophysical Union*,
1636 *89*(10), 93. Retrieved 2021-06-18, from [http://doi.wiley.com/10.1029/](http://doi.wiley.com/10.1029/2008EO100001)
1637 2008EO100001 doi: 10.1029/2008EO100001
- 1638 Leonard, L., & Duffy, C. (2016, April). Visualization workflows for level-12 HUC
1639 scales: Towards an expert system for watershed analysis in a distributed com-
1640 puting environment. *Environmental Modelling & Software*, *78*, 163–178.
1641 Retrieved 2021-02-17, from [https://linkinghub.elsevier.com/retrieve/](https://linkinghub.elsevier.com/retrieve/pii/S1364815216300019)
1642 pii/S1364815216300019 doi: 10.1016/j.envsoft.2016.01.001
- 1643 Leonard, L., & Duffy, C. J. (2013, December). Essential Terrestrial Vari-
1644 able data workflows for distributed water resources modeling. *Environ-*
1645 *mental Modelling & Software*, *50*, 85–96. Retrieved 2021-02-17, from
1646 <https://linkinghub.elsevier.com/retrieve/pii/S1364815213001941>
1647 doi: 10.1016/j.envsoft.2013.09.003
- 1648 Leonard, L., & Duffy, C. J. (2014, November). Automating data-model work-
1649 flows at a level 12 HUC scale: Watershed modeling in a distributed comput-
1650 ing environment. *Environmental Modelling & Software*, *61*, 174–190. Re-
1651 trieved 2021-02-17, from [https://linkinghub.elsevier.com/retrieve/pii/](https://linkinghub.elsevier.com/retrieve/pii/S1364815214002230)
1652 S1364815214002230 doi: 10.1016/j.envsoft.2014.07.015
- 1653 Leonard, L., Miles, B., Heidari, B., Lin, L., Castronova, A. M., Minsker, B., ...
1654 Band, L. E. (2019, January). Development of a participatory Green Infrastruc-
1655 ture design, visualization and evaluation system in a cloud supported jupyter
1656 notebook computing environment. *Environmental Modelling & Software*, *111*,
1657 121–133. Retrieved 2022-10-11, from [https://linkinghub.elsevier.com/](https://linkinghub.elsevier.com/retrieve/pii/S1364815217308290)
1658 retrieve/pii/S1364815217308290 doi: 10.1016/j.envsoft.2018.10.003
- 1659 Liang, X., Lettenmaier, D. P., Wood, E. F., & Burges, S. J. (1994). A simple hy-
1660 drologically based model of land surface water and energy fluxes for general
1661 circulation models. *Journal of Geophysical Research*, *99*, 14415–14428.
- 1662 Lin, P., Pan, M., Beck, H. E., Yang, Y., Yamazaki, D., Frasson, R., ... Wood, E. F.
1663 (2019, August). Global Reconstruction of Naturalized River Flows at 2.94
1664 Million Reaches. *Water Resources Research*, *55*(8), 6499–6516. Retrieved 2021-
1665 02-03, from <https://onlinelibrary.wiley.com/doi/10.1029/2019WR025287>
1666 doi: 10.1029/2019WR025287
- 1667 Lindström, G., Pers, C., Rosberg, J., Strömqvist, J., & Arheimer, B. (2010, June).
1668 Development and testing of the HYPE (Hydrological Predictions for the Envi-
1669 ronment) water quality model for different spatial scales. *Hydrology Research*,
1670 *41*(3-4), 295–319. Retrieved 2022-06-02, from [https://iwaponline.com/](https://iwaponline.com/hr/article/41/3-4/295/822/Development-and-testing-of-the-HYPE-Hydrological)
1671 hr/article/41/3-4/295/822/Development-and-testing-of-the-HYPE
1672 -Hydrological doi: 10.2166/nh.2010.007
- 1673 McMillan, H. K. (2021, January). A review of hydrologic signatures and
1674 their applications. *WIREs Water*, *8*(1). Retrieved 2021-04-27, from
1675 <https://onlinelibrary.wiley.com/doi/10.1002/wat2.1499> doi:
1676 10.1002/wat2.1499

- 1677 Melsen, L. A., Torfs, P. J. J. F., Uijlenhoet, R., & Teuling, A. J. (2017, March).
 1678 Comment on “Most computational hydrology is not reproducible, so is it
 1679 really science?” by Christopher Hutton et al.: REPRODUCING COMPUTA-
 1680 TIONAL STUDIES. *Water Resources Research*, *53*(3), 2568–2569. Retrieved
 1681 2021-06-18, from <http://doi.wiley.com/10.1002/2016WR020208> doi:
 1682 10.1002/2016WR020208
- 1683 Messenger, M. L., Lehner, B., Grill, G., Nedeva, I., & Schmitt, O. (2016, Decem-
 1684 ber). Estimating the volume and age of water stored in global lakes using a
 1685 geo-statistical approach. *Nature Communications*, *7*(1), 13603. Retrieved
 1686 2021-11-03, from <http://www.nature.com/articles/ncomms13603> doi:
 1687 10.1038/ncomms13603
- 1688 Miles, B. (2014). *SMALL-SCALE RESIDENTIAL STORMWATER MANAGE-
 1689 MENT IN URBANIZED WATERSHEDS: A GEOINFORMATICS-DRIVEN
 1690 ECOHYDROLOGY MODELING APPROACH* (Unpublished doctoral dis-
 1691 sertation). A dissertation submitted to the faculty at the University of North
 1692 Carolina at Chapel Hill, Chapel Hill 2014.
- 1693 Miles, B., & Band, L. E. (2015). Ecohydrology Models without Borders?: Using
 1694 Geospatial Web Services in EcohydroLib Workflows in the United States
 1695 and Australia. In R. Denzer, R. M. Argent, G. Schimak, & J. Hřebíček
 1696 (Eds.), *Environmental Software Systems. Infrastructures, Services and Ap-
 1697 plications* (Vol. 448, pp. 311–320). Cham: Springer International Publish-
 1698 ing. Retrieved 2021-06-20, from [http://link.springer.com/10.1007/
 1699 978-3-319-15994-2_31](http://link.springer.com/10.1007/978-3-319-15994-2_31) (Series Title: IFIP Advances in Information and
 1700 Communication Technology) doi: 10.1007/978-3-319-15994-2_31
- 1701 Miles, B., Leonard, L., & Blodgett, D. (2022). *EcohydroLib*. Retrieved 2022-07-13,
 1702 from <https://github.com/selinnairb/EcohydroLib>
- 1703 Minder, J. R., Mote, P. W., & Lundquist, J. D. (2010, July). Surface temper-
 1704 ature lapse rates over complex terrain: Lessons from the Cascade Moun-
 1705 tains. *Journal of Geophysical Research*, *115*(D14), D14122. Retrieved
 1706 2021-03-17, from <http://doi.wiley.com/10.1029/2009JD013493> doi:
 1707 10.1029/2009JD013493
- 1708 Mizukami, N., Clark, M. P., Gharari, S., Kluzek, E., Pan, M., Lin, P., ... Ya-
 1709 mazaki, D. (2021, June). A Vector-Based River Routing Model for Earth
 1710 System Models: Parallelization and Global Applications. *Journal of Ad-
 1711 vances in Modeling Earth Systems*, *13*(6). Retrieved 2021-11-02, from
 1712 <https://onlinelibrary.wiley.com/doi/10.1029/2020MS002434> doi:
 1713 10.1029/2020MS002434
- 1714 Mizukami, N., Clark, M. P., Sampson, K., Nijssen, B., Mao, Y., McMillan, H.,
 1715 ... Brekke, L. D. (2016, June). mizuRoute version 1: a river network
 1716 routing tool for a continental domain water resources applications. *Geo-
 1717 scientific Model Development*, *9*(6), 2223–2238. Retrieved 2021-02-03,
 1718 from <https://gmd.copernicus.org/articles/9/2223/2016/> doi:
 1719 10.5194/gmd-9-2223-2016
- 1720 Mizukami, N., Rakovec, O., Newman, A. J., Clark, M. P., Wood, A. W., Gupta,
 1721 H. V., & Kumar, R. (2019, June). On the choice of calibration metrics for
 1722 “high-flow” estimation using hydrologic models. *Hydrology and Earth System
 1723 Sciences*, *23*(6), 2601–2614. Retrieved from [https://www.hydrol-earth-syst-
 1724 -sci.net/23/2601/2019/](https://www.hydrol-earth-syst-sci.net/23/2601/2019/) doi: 10.5194/hess-23-2601-2019
- 1725 Murphy, A. H. (1988). Skill Scores Based on the Mean Square Error and Their Re-
 1726 lationships to the Correlation Coefficient. *MONTHLY WEATHER REVIEW*,
 1727 *116*, 2417–2424. doi: [https://doi.org/10.1175/1520-0493\(1988\)116%3C2417:
 1728 SSBOTM%3E2.0.CO;2](https://doi.org/10.1175/1520-0493(1988)116%3C2417:SSBOTM%3E2.0.CO;2)
- 1729 Nash, J., & Sutcliffe, J. (1970, April). River flow forecasting through conceptual
 1730 models part I — A discussion of principles. *Journal of Hydrology*, *10*(3), 282–
 1731 290. Retrieved from <https://linkinghub.elsevier.com/retrieve/pii/>

- 1732 0022169470902556 doi: 10.1016/0022-1694(70)90255-6
 1733 NCAR Research Applications Laboratory | RAL. (2021). *Noah-*
 1734 *Multiparameterization Land Surface Model (Noah-MP LSM)*. Retrieved
 1735 2021-11-15, from [https://ral.ucar.edu/solutions/products/noah-](https://ral.ucar.edu/solutions/products/noah-multiparameterization-land-surface-model-noah-mp-lsm)
 1736 [multiparameterization-land-surface-model-noah-mp-lsm](https://ral.ucar.edu/solutions/products/noah-multiparameterization-land-surface-model-noah-mp-lsm)
 1737 Olden, J. D., & Poff, N. L. (2003). Redundancy and the choice of hydrologic indices
 1738 for characterizing streamflow regimes. *River Research and Applications*, 19(2),
 1739 101–121. (ISBN: 15351459 (ISSN)) doi: 10.1002/rra.700
 1740 Pietroniro, A., Fortin, V., Kouwen, N., Neal, C., Turcotte, R., Davison, B., ...
 1741 Pellerin, P. (2007, May). Development of the MESH modelling system for hy-
 1742 drological ensemble forecasting of the Laurentian Great Lakes at the regional
 1743 scale. *Hydrology and Earth System Sciences*, 11(4), 1279–1294. Retrieved
 1744 2021-04-20, from <https://hess.copernicus.org/articles/11/1279/2007/>
 1745 doi: 10.5194/hess-11-1279-2007
 1746 Pushpalatha, R., Perrin, C., Moine, N. L., & Andréassian, V. (2012, February). A
 1747 review of efficiency criteria suitable for evaluating low-flow simulations. *Jour-*
 1748 *nal of Hydrology*, 420-421, 171–182. (Publisher: Elsevier B.V.) doi: 10.1016/
 1749 j.jhydrol.2011.11.055
 1750 QGIS Development Team. (2021). *QGIS Geographic Information System*. QGIS As-
 1751 sociation. Retrieved from <https://www.qgis.org/>
 1752 Samaniego, L., Kumar, R., & Attinger, S. (2010). Multiscale parameter regionaliza-
 1753 tion of a grid-based hydrologic model at the mesoscale. *Water Resources Re-*
 1754 *search*, 46(5), 1–25. doi: 10.1029/2008WR007327
 1755 Sandve, G. K., Nekrutenko, A., Taylor, J., & Hovig, E. (2013, October). Ten Simple
 1756 Rules for Reproducible Computational Research. *PLoS Computational Biology*,
 1757 9(10), e1003285. Retrieved 2021-07-15, from [https://dx.plos.org/10.1371/](https://dx.plos.org/10.1371/journal.pcbi.1003285)
 1758 [journal.pcbi.1003285](https://dx.plos.org/10.1371/journal.pcbi.1003285) doi: 10.1371/journal.pcbi.1003285
 1759 Sazib, N. S. (2016). *Physically Based Modeling of the Impacts of Climate Change*
 1760 *on Streamflow Regime* (Doctoral dissertation, A dissertation submitted to
 1761 the faculty at the University of North Carolina at Chapel Hill, Utah State
 1762 University). doi: 10.26076/7BBE-E62D
 1763 Sen Gupta, A., Tarboton, D., Hummel, P., Brown, M., & Habib, S. (2015, June).
 1764 Integration of an energy balance snowmelt model into an open source mod-
 1765 eling framework. *Environmental Modelling & Software*, 68, 205–218. Re-
 1766 trieved 2021-06-19, from [https://linkinghub.elsevier.com/retrieve/pii/](https://linkinghub.elsevier.com/retrieve/pii/S1364815215000663)
 1767 [S1364815215000663](https://linkinghub.elsevier.com/retrieve/pii/S1364815215000663) doi: 10.1016/j.envsoft.2015.02.017
 1768 Slater, L. J., Thirel, G., Harrigan, S., Delaigue, O., Hurley, A., Khouakhi, A., ...
 1769 Smith, K. (2019, July). Using R in hydrology: a review of recent developments
 1770 and future directions. *Hydrology and Earth System Sciences*, 23(7), 2939–2963.
 1771 Retrieved 2021-02-17, from [https://hess.copernicus.org/articles/23/](https://hess.copernicus.org/articles/23/2939/2019/)
 1772 [2939/2019/](https://hess.copernicus.org/articles/23/2939/2019/) doi: 10.5194/hess-23-2939-2019
 1773 Stagge, J. H., Rosenberg, D. E., Abdallah, A. M., Akbar, H., Attallah, N. A., &
 1774 James, R. (2019, March). Assessing data availability and research reproducibil-
 1775 ity in hydrology and water resources. *Scientific Data*, 6(1), 190030. Retrieved
 1776 2021-02-17, from <http://www.nature.com/articles/sdata201930> doi:
 1777 10.1038/sdata.2019.30
 1778 Stodden, V., & Miguez, S. (2013). Best Practices for Computational Science:
 1779 Software Infrastructure and Environments for Reproducible and Extens-
 1780 sible Research. *SSRN Electronic Journal*. Retrieved 2021-02-17, from
 1781 <http://www.ssrn.com/abstract=2322276> doi: 10.2139/ssrn.2322276
 1782 Sulla-Menashe, D., & Friedl, M. A. (2018). *User Guide to Collection 6 MODIS*
 1783 *Land Cover (MCD12Q1 and MCD12C1) Product* (User Guide). Retrieved from
 1784 https://lpdaac.usgs.gov/documents/101/MCD12_User_Guide_V6.pdf
 1785 Sulla-Menashe, D., Gray, J. M., Abercrombie, S. P., & Friedl, M. A. (2019, March).
 1786 Hierarchical mapping of annual global land cover 2001 to present: The MODIS

- 1787 Collection 6 Land Cover product. *Remote Sensing of Environment*, 222,
1788 183–194. Retrieved 2021-06-17, from [https://linkinghub.elsevier.com/
1789 retrieve/pii/S0034425718305686](https://linkinghub.elsevier.com/retrieve/pii/S0034425718305686) doi: 10.1016/j.rse.2018.12.013
- 1790 Tadono, T., Nagai, H., Ishida, H., Oda, F., Naito, S., Minakawa, K., & Iwamoto,
1791 H. (2016, June). GENERATION OF THE 30 M-MESH GLOBAL DIGITAL
1792 SURFACE MODEL BY ALOS PRISM. *ISPRS - International Archives of
1793 the Photogrammetry, Remote Sensing and Spatial Information Sciences*, XLI-
1794 B4, 157–162. Retrieved 2021-06-12, from [http://www.int-arch-photogramm-
1795 -remote-sens-spatial-inf-sci.net/XLI-B4/157/2016/isprs-archives
1796 -XLI-B4-157-2016.pdf](http://www.int-arch-photogramm-remote-sens-spatial-inf-sci.net/XLI-B4/157/2016/isprs-archives-XLI-B4-157-2016.pdf) doi: 10.5194/isprsarchives-XLI-B4-157-2016
- 1797 Tang, G., Clark, M. P., Papalexiou, S. M., Ma, Z., & Hong, Y. (2020, April). Have
1798 satellite precipitation products improved over last two decades? A comprehen-
1799 sive comparison of GPM IMERG with nine satellite and reanalysis datasets.
1800 *Remote Sensing of Environment*, 240, 111697. Retrieved 2021-06-17, from
1801 <https://linkinghub.elsevier.com/retrieve/pii/S0034425720300663>
1802 doi: 10.1016/j.rse.2020.111697
- 1803 Tarboton, D. G., Horsburgh, J. S., Maidment, D. R., Whiteaker, T., Zaslavsky, I.,
1804 Piasecki, M., ... Whitenack, T. (2009). Development of a community hydro-
1805 logic information system. In (pp. 988–994). Modelling and Simulation Society
1806 of Australia and New Zealand and International Association for Mathematics
1807 and Computers in Simulation.
- 1808 Tesfa, T. K., Tarboton, D. G., Watson, D. W., Schreuders, K. A., Baker, M. E.,
1809 & Wallace, R. M. (2011, December). Extraction of hydrological prox-
1810 imity measures from DEMs using parallel processing. *Environmental
1811 Modelling & Software*, 26(12), 1696–1709. Retrieved 2021-11-23, from
1812 <https://linkinghub.elsevier.com/retrieve/pii/S1364815211001794>
1813 doi: 10.1016/j.envsoft.2011.07.018
- 1814 Tiesinga, E., Mohr, P. J., Newell, D. B., & Taylor, B. N. (2019). *The 2018 CO-
1815 DATA Recommended Values of the Fundamental Physical Constants*. Gaithers-
1816 burg, MD 20899: National Institute of Standards and Technology. Retrieved
1817 2021-10-11, from <http://physics.nist.gov/constants>
- 1818 U.S. Department of Agriculture: Agricultural Research Service (USDA ARS).
1819 (2021). *ROSETTA Class Average Hydraulic Parameters*. Retrieved 2021-
1820 11-15, from [https://www.ars.usda.gov/pacific-west-area/riverside-ca/
1821 agricultural-water-efficiency-and-salinity-research-unit/docs/
1822 model/rosetta-class-average-hydraulic-parameters/](https://www.ars.usda.gov/pacific-west-area/riverside-ca/agricultural-water-efficiency-and-salinity-research-unit/docs/model/rosetta-class-average-hydraulic-parameters/)
- 1823 Vanderborght, J., Kasteel, R., Herbst, M., Javaux, M., Thiéry, D., Vanclooster, M.,
1824 ... Vereecken, H. (2005). A Set of Analytical Benchmarks to Test Numerical
1825 Models of Flow and Transport in Soils. *Vadose Zone Journal*, 4(1), 206.
1826 Retrieved 2021-06-12, from [https://www.soils.org/publications/vzj/
1827 abstracts/4/1/0206](https://www.soils.org/publications/vzj/abstracts/4/1/0206) doi: 10.2136/vzj2005.0206
- 1828 Vanderkelen, I., Gharari, S., Mizukami, N., Clark, M. P., Lawrence, D. M., Swenson,
1829 S., ... Thiery, W. (2022, June). Evaluating a reservoir parametrization in the
1830 vector-based global routing model mizuRoute (v2.0.1) for Earth system model
1831 coupling. *Geoscientific Model Development*, 15(10), 4163–4192. Retrieved
1832 2022-07-25, from [https://gmd.copernicus.org/articles/15/4163/2022/
1833 doi: 10.5194/gmd-15-4163-2022](https://gmd.copernicus.org/articles/15/4163/2022/)
- 1834 Vorobevskii, I. (2022, May). *hydrovorobey/Global_brook90: zonedo*. Zenodo. Re-
1835 trieved 2022-07-13, from <https://zenodo.org/record/6535132> doi: 10.5281/
1836 ZENODO.6535132
- 1837 Vorobevskii, I., Kronenberg, R., & Bernhofer, C. (2020, July). Global BROOK90
1838 R Package: An Automatic Framework to Simulate the Water Balance at
1839 Any Location. *Water*, 12(7), 2037. Retrieved 2021-04-25, from [https://
1840 www.mdpi.com/2073-4441/12/7/2037](https://www.mdpi.com/2073-4441/12/7/2037) doi: 10.3390/w12072037
- 1841 Wallace, J. M., & Hobbs, P. V. (2006). *Atmospheric science: an introductory sur-*

- 1842 *vey* (2nd ed ed.) (No. v. 92). Amsterdam ; Boston: Elsevier Academic Press.
 1843 (OCLC: ocm62421169)
- 1844 Weiler, M., & Beven, K. (2015, September). Do we need a Community Hydrological
 1845 Model?: DO WE NEED A COMMUNITY HYDROLOGICAL MODEL? *Wa-*
 1846 *ter Resources Research*, *51*(9), 7777–7784. Retrieved 2021-06-19, from [http://](http://doi.wiley.com/10.1002/2014WR016731)
 1847 doi.wiley.com/10.1002/2014WR016731 doi: 10.1002/2014WR016731
- 1848 Wi, S., Ray, P., Demaria, E. M., Steinschneider, S., & Brown, C. (2017, Decem-
 1849 ber). A user-friendly software package for VIC hydrologic model development.
 1850 *Environmental Modelling & Software*, *98*, 35–53. Retrieved 2022-10-14, from
 1851 <https://linkinghub.elsevier.com/retrieve/pii/S1364815216308131>
 1852 doi: 10.1016/j.envsoft.2017.09.006
- 1853 Wilkinson, M. D., Dumontier, M., Aalbersberg, I. J., Appleton, G., Axton, M.,
 1854 Baak, A., ... Mons, B. (2016, December). The FAIR Guiding Principles for
 1855 scientific data management and stewardship. *Scientific Data*, *3*(1), 160018.
 1856 Retrieved 2021-02-17, from <http://www.nature.com/articles/sdata201618>
 1857 doi: 10.1038/sdata.2016.18
- 1858 World Meteorological Organization. (2017). *Guide to the Implementation of Quality*
 1859 *Management Systems for National Meteorological and Hydrological Services*
 1860 *and Other Relevant Service Providers* (Tech. Rep. No. WMO-No. 1100).
- 1861 Xu, X., Frey, S. K., Boluwade, A., Erler, A. R., Khader, O., Lapen, D. R., &
 1862 Sudicky, E. (2019, August). Evaluation of variability among differ-
 1863 ent precipitation products in the Northern Great Plains. *Journal of*
 1864 *Hydrology: Regional Studies*, *24*, 100608. Retrieved 2021-06-17, from
 1865 <https://linkinghub.elsevier.com/retrieve/pii/S2214581818303410>
 1866 doi: 10.1016/j.ejrh.2019.100608
- 1867 Yamazaki, D., Ikeshima, D., Sosa, J., Bates, P. D., Allen, G. H., & Pavelsky, T. M.
 1868 (2019, June). MERIT Hydro: A High-Resolution Global Hydrography Map
 1869 Based on Latest Topography Dataset. *Water Resources Research*, *55*(6), 5053–
 1870 5073. Retrieved 2021-02-03, from [https://onlinelibrary.wiley.com/doi/](https://onlinelibrary.wiley.com/doi/10.1029/2019WR024873)
 1871 [10.1029/2019WR024873](https://onlinelibrary.wiley.com/doi/10.1029/2019WR024873) doi: 10.1029/2019WR024873
- 1872 Yamazaki, D., Ikeshima, D., Tawatari, R., Yamaguchi, T., O’Loughlin, F., Neal,
 1873 J. C., ... Bates, P. D. (2017, June). A high-accuracy map of global terrain
 1874 elevations: Accurate Global Terrain Elevation map. *Geophysical Research Let-*
 1875 *ters*, *44*(11), 5844–5853. Retrieved 2021-06-12, from [http://doi.wiley.com/](http://doi.wiley.com/10.1002/2017GL072874)
 1876 [10.1002/2017GL072874](http://doi.wiley.com/10.1002/2017GL072874) doi: 10.1002/2017GL072874